Characterization and optimization of *Rhodosporidium toruloides* for production of lipids

Niharika Singh

Department of Chemical Engineering

Lund University, 2021

Characterization and optimization of *Rhodosporidium toruloides* for production of lipids

Master thesis

by

Niharika Singh

Department of Chemical Engineering

Lund University

May, 2021

Supervisor: Henrik Almqvist

Examiner: Gunnar Lidén

ABSTRACT

Oleaginous microorganisms provide an opportunity to produce oils without the use of arable land for cultivation of oil-containing plants. Oleaginous microorganisms are also capable of storing products of pharmaceutical interest alongside storing polymers, which could open new opportunities in the bioplastic industry. Oily yeasts have several advantages in comparison to alternatives; their doubling times are shorter than that of plant cells; their resistance to environmental changes is than those of bacteria, and they grow as single cells as opposed to (other) fungi. In this study, *Rhodosporidium toruloides* strain BOT A-2 was characterized to select the best carbon source, temperature, and pH requirements for maximal lipid accumulation. Specific growth rates of ~0.2 h^{-1} were measured at optimal growth conditions of 30°C temperature, pH of 5.5, and glucose as the carbon source. Different C:N ratios were evaluated (20, 40, 80, and 100) to determine the value giving the highest titer of lipids. Of the process parameters tested, a C:N ratio of 80 and glucose concentration of 50 g/L was selected for batch experiments and 20 g/L of glucose for the fed-batch experiment. Batch and fed-batch mode resulted in a lipid accumulation of about 40 %(w/w) of the cell dry weight. The lipid profile showed a dominance of unsaturated C-16:0 fatty acids at higher C:N ratios. Further investigation of lipid accumulation was done using flow cytometry, and it was clearly shown that cells grow in size in the later stages of fermentation due to lipid accumulation. The experimental results were compared to predictions made using the flux balance analysis software OptFlux, to assess the capability of the model in predicting results.

POPULAR ABSTRACT

This thesis was based on *Rhodosporidium toruloides* a super pink, super oily yet super useful species of yeasts! This thesis resulted in the yeasts storing about 40% of the cell mass as oils also known as lipids. The storage capability of these yeasts is what resulted in them being called oleaginous yeasts. How do they accumulate lipids you ask? Simple, they channel all the extra sugar one feeds them when you starve them of an essential nutrient such as nitrogen. The research here focuses on finding which sugar was the best at which temperature and at what pH do these cells grow the best. Once those conditions were selected, the process was then scaled up from shake flask to reactors. The main end goal was to see how well these pink yeasts store lipids.

Rhodosporidium toruloides are yeasts that can store lipids hence are termed as oleaginous. For a microorganism to be termed as "oleaginous", they should be able to store at least 20% of their cell mass as lipids. As mentioned in the introduction, these yeasts need to be starved of an essential nutrient namely nitrogen, sulfur, or phosphate; in this research nitrogen was the preferred nutrient. Before the cells were starved, the best growth conditions were decided. The first condition was to check which sugar was taken up readily amongst glucose, glycerol, and xylose. As it turns out this yeast can grow in all of them, but it is faster in glucose and xylose compared to glycerol. This can be interesting as if this process were to be industrialized it is important for the price of the sugar to be affordable, and glucose is a pretty expensive sugar! So, in situations like this, a source like glycerol which is a by-product of many other industrial processes such as manufacturing of biodiesel could lead to a beneficial process economy. The second condition was temperature, previous research suggested we use 30°C as the growth temperature. So, to verify that claim the research checked the growth of the yeast in 27, 33, and 36°C. The results once again showed that our pink yeast is quite strong and is capable of growing at all those temperatures just at different speeds. The cells preferred 27°C as the most comfortable condition, thereby reassuring the above-mentioned claim. The third and final condition was checking the best-suited pH, which is a measure of whether the yeasts prefer an acidic, basic, or neutral growth media environment. Previous research once again suggested a pH of 5.5 to check whether that was true for our yeasts, we grew it in pH 4.0, 4.5, and 6.5. The change in pH can lead to the cells experiencing stress. The yeasts once again showed that it is very strong and can grow in all conditions of stress, but it is the most comfortable in pH 6.5. So, the final conditions to grow the yeasts were set at glucose (the sugar source), 30°C (temperature source), and 5.5 (pH source).

Once the yeasts grew well the starvation process to produce lipids were tested, but to produce lipid, one must decide what ratio of sugar to nitrogen they want to use? That ratio is called C:N ratio, where C:N stands for carbon (the sugar) and nitrogen ratio that is put in the growth medium. The ratios tested were 20, 40,80, and 100. The yeasts showed no significant storage at C:N of 20, showed about 20% storage at C:N 40, around 35% storage at C:N 80, and 40% storage at C:N 100. The C:N experiments were initially performed in 300 mL shake flasks to check which ratio gives more lipids, and then scaled up to check if the cells could store more lipids in a more controlled environment which a reactor can provide. A C:N ratio of 80 was chosen as it did not put the cells under too much stress.

The reactor experiments were separated in two categories: (i) Batch- this means throwing in everything in the reactor at once and just waiting for the cells to become pink and consume all of the sugar; (ii) Fed-Batch- in this category the cells are given a little sugar so they can grow well until the nitrogen

gets completely used up, once the nitrogen is used up they are fed sugar little by little until they store as much lipids as they can. The batch experiments resulted in the cells storing 35% of their cell mass as lipids, but the experiment can only run for 72 hours as the cells completely consume the sugar. The fed-batch experiments resulted in ~37% of their cell mass as lipids but they continued to store lipids for 192 hours. Now, one would start to think how is that the experiment runs longer yet the amount lipids has not increased much? Well, there were more lipids, but they were no longer in the yeasts. The lipids were in the growth medium, how you ask? The pink yeasts burst! Yes, burst because they stored more lipids than they could handle. Another observation we made was that the cells grew in size as the experiment progressed, this is possible because the nitrogen starvation doesn't allow them to divide but the excess sugar that is getting stored as lipids increase the size.

To conclude, *Rhodosporidium toruloides* have a bright (pink) future in this area of research! Who knows, maybe some time from now they would be able to store plastics?

ACKNOWLEDGEMENT

Beginning a master thesis in times of a pandemic can be very taxing, but thanks to the guidance of my supervisor Henrik Almqvist it was possible for me to complete it on time and with positive results. For being an extremely approachable person and answering all my questions with immense patience, I truly appreciate that. I would also like to extend my gratitude to my examiner Prof. Gunnar Lidén to allow me to be a part of this project and for his guidance with my research.

To my family without whom I would have not stepped out of my comfort zone and flown a long way from home. I would also like to mention all the friends I have made thanks to Sweden, for making sure I remained motivated to complete my studies here. So, thank you Chia-Yin, Manuel, Mirac, Sharmeen, Virginia, Yara, and Zixuan.

I would also like to extend my gratitude to the department of chemical engineering for their warmth in the duration of my thesis. A special thanks to Joana, Astrid, and Loren for their presence in the department and fika room discussions, it made coming to work all the more exciting. I would also like to extend my thanks to the RhoBot group Marie, Daniel, and Tova for their insightful input and their encouragement towards my research.

I would like to thank my two opponents Jack and Tushar for reading and appreciating my work.

TABLE OF CONTENTS

INTRODUCTION & AIM

The ability of the microorganism to accumulate lipids as single cells oils has gained interest, as plant oils take up arable land which can be used otherwise. Microorganisms such as bacteria, fungi, and yeasts are capable of accumulating lipids but yeasts were the main area of interest in this study due to their ease of scale-up, faster doubling times in comparison to plants, ability to take up multiple carbon sources, and sustain a wide range of temperatures and pHs (Ageitos *et al.*, 2011). Oleaginous microorganisms are defined as microorganisms that can accumulate more than 20% of their cell dry weight as oils (Papanikolaou and Aggelis, 2011). Oily yeasts have been reported to store carbon in the form of triacylglycerols (TAGs), which are polyunsaturated fatty acids (PFAs), as opposed to bacteria which are known to store specialized polyesters such as polyhydroxyalkanoates (PHAs) (Ratledge 1994; Steinbüchel 1991). The lipids accumulated by these organisms are also known as single-cell oils (SCOs) and have opened new avenues for research in the renewable chemicals sector. SCOs find applications as a potential substitute for cocoa butter, as a source of omega-3 eicosapentaenoic acid supplements, and many other nutraceuticals (Ratledge & Wynn, 2002; Xie *et al.*, 2015). The lipid biosynthesis in oleaginous microorganisms provides a strong base in the production of other fatty acid based products, an example of which is biodiesel (Shi & Zhao, 2017; Nawabi *et al*., 2011). The produced lipids can be converted into fatty acid methyl esters (FAME) with ease (Blazeck *et al*., 2014).

This study aims at characterizing the production process of an oily yeast, *Rhodosporidium toruloides*, a basidiomycete, which has been previously reported to accumulate up to 70% of its cell dry weight as lipids (Ageitos *et al*., 2011). In the current work, the strain *Rhodosporidium toruloides* BOT A-2 was characterized based on: (i) Preferred carbon source between glucose, glycerol, and xylose; (ii) preferred cultivation temperature in the 27-36°C range; and (iii) preferred cultivation pH in the 4.0-6.5 range. Once the cultivation conditions were characterized, the lipid accumulation at different carbon to nitrogen molar ratios of 20, 40, 80, and 100 was measured. The previous experiments were then scaled up from shake-flasks (25mL) to bioreactors (1L) with batch and fed-batch feeding strategies, to check for lipid accumulation at larger volumes. Furthermore, a flux analysis software, OptFlux, was used together with a published metabolic model of R. toruloides, to make in silico predictions of anticipated product yields in the aforementioned experiments in order to assess the applicability of the model for predicting yields.

Background

Lipid synthesis

Accumulation of lipids as triacylglycerols, TAGs, takes place in certain microorganisms which undergo nitrogen, phosphate, or sulfur (this study focuses on nitrogen) limitation in the presence of excess carbon. These conditions allow the channelling of excess carbon into lipid synthesis. The accumulation in oily yeasts is possible due to their ability to provide a continuous supply of acetyl-CoA and NADPH into the cytosol where the acetyl-CoA in the cytosol is the precursor for fatty acid synthetase (FAS) and the NADPH acts as a reductant in lipid synthesis. The acetyl-CoA formation in oleaginous yeasts takes place through the action of ATP: citrate lyase (ACL), (Ratledge 2004). The lipid formation process can be further understood by fig. 1. The lipid biosynthesis takes place in both the cytosol and the mitochondria, the process begins with the onset of nitrogen limitation. The lack of nitrogen affects the concentration of adenosine monophosphate (AMP), whose concentration is regulated by the enzyme AMP deaminase. The concentration of AMP deaminase is up-regulated during the nitrogen limitation and leads to halting of the TCA cycle. The halting of the TCA further leads to inhibition of the enzyme isocitrate dehydrogenase (ICDH), which leads to accumulation of isocitrate which is converted to citrate with the help of aconitase enzyme. The microorganisms have an effective citrate flux which shuttles the excess citrate from the mitochondria to the cytoplasm, where the ACL cleaves it to Acetyl-CoA and oxaloacetate. The acetyl-CoA further gets converted to TAG in the presence of FAS (Ratledge,2004). The NADPH part of this metabolic "ecosystem" is derived from the malate shuttle, which is governed by malic enzyme. The malic enzyme is important for shuttling NADPH as the membrane-bound variant allows for channelling of the excess carbon into lipid synthesis. Without the presence of this membrane-bound malic enzyme, oleaginous microorganisms would only be able to produce essential phospholipids, not storage lipids (Ratledge & Wynn, 2002).

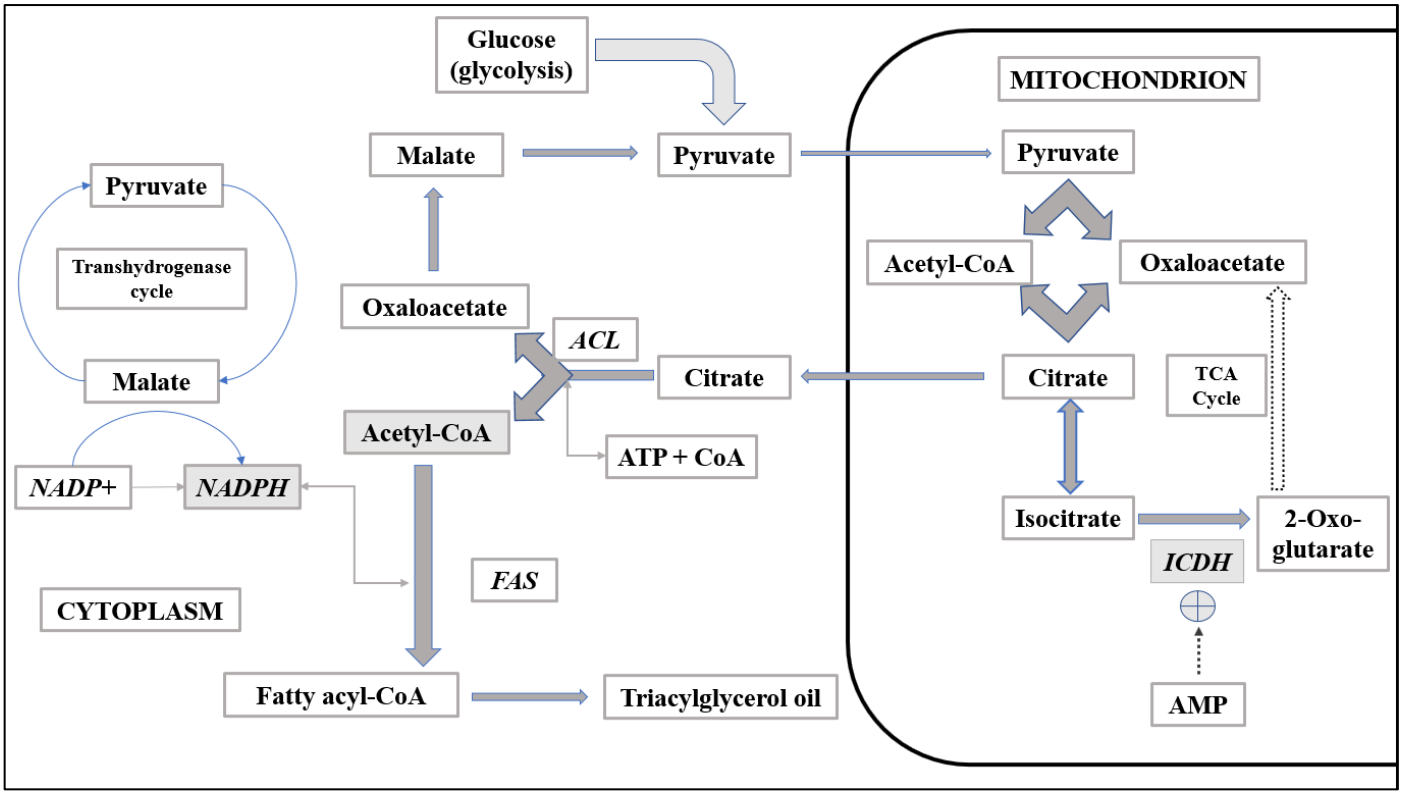

Fig 1: Lipid biosynthesis scheme in oleaginous yeasts (adapted from Ratledge & Wynn, 2002). Note- Cytoplasm: ACL: ATP Citrate Lyase, FAS- Fatty Acid synthase; Mitochondria: ICDH- Isocitrate dehydrogenase, AMP- Adenosine monophosphate.

Modelling of metabolism

Optflux is a user-friendly open-source in silico metabolic engineering software aimed to aid strain optimization by identifying targets for metabolic engineering using various algorithms. It also allows simulation of phenotypes for wild-type and mutants by using flux balance analysis (Rocha *et al*., 2010). Flux balance analysis (FBA) is a mathematical approach for studying the genome-scale biochemical pathways. By applying an optimization criterion, e.g. maximized growth given specified uptake rates, it allows calculation of specific growth rates and production rates of important metabolites such as TAGs, from the calculating the flow of metabolites through metabolic networks (Orth *et al*., 2010). In this thesis, OptFlux was used to simulate the specific growth rates and TAG yields under different C:N molar ratios. The OptFlux model designed by Castañeda *et al*. was used, the model calculates fluxes for TAG production depending on the entry carbon source. The model utilizes the cell mass equation as illustrated in fig. 2, and the model includes pathways for glycolysis, pentose phosphate pathway, TCA cycle, and glyoxylate cycle; these cycles are available for four carbon sources namely glucose, glycerol, xylose, and arabinose (Castañeda *et al*.,2018). OptFlux in this study will be used to predict

the optimal conditions for lipid production and the simulated values will be compared to the experimental data and the models usefulness for this particular strain will be assessed.

Cell mass equation	**254.0*M_ATP_C + 254.0*M_H2O_C + 6.0*M_3_PG_C + 6.2*M_PEP_C + 10.0*M_OAA_C + 90.0*M_NADPH_C + 16.0*M_H_M + 51.9*M_GLUT_C + M_GLYC3P_C + 16.0*M_NAD_C + 4.5*M_F6P_C + 25.0*M_G6P_C + 18.0*M_PYR_C + 22.0*M_NADPH_M + 11.0*M_AKG_M + 3.0*M_ACCOA_M + 24.0*M_ACCOA_C + 6.0*M_NAD_M + 4.6*M_GLUM_C + 3.2*M_R5P_C + 1.53*M_H2S_C + 3.2*M_E4P_C**	→ **254.0*M_PI_C + 254.0*M_ADP_C + 90.0*M_NADP_C + 180.0*M_H_C + 16.0*M_NADH_C + 22.0*M_NADP_M + 24.0*M_COA_C + 3.0*M_COA_M + 10.0*M_CELL_MASS_C + 6.0*M_NADH_M**

Fig. 2: Cell mass equation for the Optflux metabolic model (Castañeda *et al.*,2018).

MATERIALS & METHODS

Seed Culture

Rhodosporidum toruloides strain BOT A-2 was obtained from the Department of Biology and Biological Engineering, Food Science Division, Chalmers University of Technology. The yeasts for the experiment were grown in Yeast Extract–Peptone–Dextrose (YPD) Medium at a peptone concentration of 20 g/L, glucose concentration of 20 g/L, and yeast extract concentration of 10 g/L. The culture medium was sterilized at 121°C for 20 min, the sugar was sterilized separately. This culture was used to inoculate shake flask and reactor experiments. Seed culture was cultivated in 25 mL of YPD medium in a cotton-stoppered 300 ml Erlenmeyer flask for 72 in an incubator at a temperature of 30°C at 180 rpm.

Fermentation

Shake flask fermentation for culture condition determination

The shake flask experiments were carried out in 300 mL Erlenmeyer flasks for characterization of sugars, pH, and temperature. The fermentation media consisted of yeast nitrogen base (YNB) without amino acids and ammonium salt at a 1.7 g/L concentration; YNB buffer containing $C_8H_5KO_4$ at 5.1 g/L and KOH at 1.1 g/L at pH 6; $(NH_4)_2SO_4$ at 10 g/L; and sugars (glucose, glycerol, and xylose) at 20 g/L. The fermentation media was sterilized at 121°C for 20 min. The sugars and ammonium sulfate were sterilized separately from the other components of the medium. The final fermentation volume in shake flasks was maintained at 25 mL with an inoculum size of 3-4% (v/v) corresponding to an initial OD_{600} of 12. The sugar characterization was carried out in a 30°C incubator at 180 rpm for 72 hours with cotton plugs to allow aeration. For pH characterization, the varying pHs of 4,5, 5.5, and 6.5 were reached using 1M HCl and 1N NaOH. For temperature characterization 27, 33, and 36°C were maintained using different incubators. All experiments were carried out in duplicates.

Shake flask fermentation for lipid production

Lipid production fermentations were carried out in 300 mL cotton plugged Erlenmeyer flasks with YNB media similar to the culture conditions experiments with the difference being in the amount of $(NH_4)_2SO_4$. The experiments followed C:N ratios of 20, 40, 80, and 100 with the amount of glucose fixed at 20 g/L (Note: The C:N ratios were calculated on a C-mole and N-mole basis). The amount of ammonium source was calculated in molar terms. The fermentation media was sterilized at 121°C for 20 min. The final fermentation volume in shake flasks was maintained at 25 mL with an inoculum size

of 3-4% (v/v) corresponding to an initial OD_{600} of 12, in a 30°C incubator at 180 rpm for 72 hours. All experiments were performed in duplicates.

Batch bioreactor fermentations

Lipid production in *Rhodosporidium toruloides* was performed in two bioreactors the Biostat CT bioreactor (B. Braun International, Melsungen, Germany) also referred to as the sterilization in place (SIP) reactor; and the Sartorius Biostat bioreactor (Sartorius Lab Instruments GmbH & Co. KG, Goettingen, Germany) also known as the old control (OC) reactor at 30°C and stirring of 400 rpm with a working volume of 1.0 L for 72 hours. The seed inoculum was maintained similar to the shake flasks at 3-4% (v/v) corresponding to an initial OD_{600} of 12. The medium was kept similar to the one in shake flasks with the only differences being the amount of glucose being increased to 50 g/L rather than the 20 g/L in the shake flasks; the YNB buffers containing $C_8H_5KO_4$ at 5.1 g/L and KOH at 1.1 g/L was replaced by 1M of H_2SO_4 and 2N of NaOH / KOH to maintain the pH at 5.5 automatically fed to the reactors by the reactor controller. The bioreactors air supply was set to 0.5 L/min as it was controlled by the pO_2 which had a threshold of 50%. The Braun Biostat CT bioreactor was sterilized in place at 121°C for 20 min while the Sartorius Biostat bioreactor was autoclaved at the same. The amount of CO_2 in the off-gas was measured using gas analyzers BlueInOne Cell (BlueSens, Herten, Germany) for the Biostat CT bioreactor and the Electrolab FerMac 368 Gas Analyser (Electrolab Biotech Limited, Gloucestershire, UK) to check for cellular respiration. The bioreactor experiments were performed in duplicates and the values obtained were compared with the ones extracted from the OptFlux software.

Cell counting was carried out for both the bioreactors at 6, 24, 48, and 72nd hours of fermentation. Counting was done using a counting chambers Bürker hemocytometer (Hirschmann Laborgeräte, Germany) which had a depth of 0.1 mm. The samples were viewed under a microscope with 40x magnification (LRI Instrument AB, Sweden). The samples were diluted depending on the fermentation time, the cell count was kept at ~60 cells per 16 cells and a hand tally counter was used and the formula used for total cell count was: $Cell\ Count = \frac{Live\ yeast\ count * DF * 10^4}{No.\ of\ squares}$.

Fed-Batch bioreactor fermentation

Fed-batch experiments had a similar procedure as the batch experiments with differences in the initial glucose concentration, which was lowered to 20 g/L. The stirring was increased to 500 rpm to avoid foaming, the cultivation temperature was maintained at 30°C. The feeding was started after 24 hours of fermentation as previous experiments indicated ammonia exhaustion at that stage. The feeding rate

was set at 2.2-2.0% pump capacity to maintain 0.7 g/h of the 400 g/L glucose stock solution. The Braun Biostat CT bioreactor was sterilized in place at 121°C for 20 min while the Sartorius Biostat bioreactor was autoclaved at the same. The amount of CO_2 in the off-gas was measured using gas analyzers BlueInOne Cell (BlueSens, Herten, Germany) for the Biostat CT bioreactor and the Electrolab FerMac 368 Gas Analyser (Electrolab Biotech Limited, Gloucestershire, UK) to check for cellular respiration. The fermentation was continued for 192 hours as the gas analyzer reflected respiring cells. Cell count and size were monitored using flow cytometry.

Analyses

Optical density and cell dry weight

Samples at the decided sampling hours were analyzed for optical density (OD) at 600 nm using a V-1200 Spectrophotometer (VWR International Europe BVBA, Leuven, Belgium). The samples were diluted in 0.9% (w/v) NaCl to maintain cell homeostasis. Cell dry weight (CDW) was measured in pre-weighed 5/15 mL glass test tubes after centrifuging samples at 10,000xg for 10 min to remove culture media. The cell pellet was then washed with distilled water and resuspended by vortexing, the procedure was repeated. The resuspended cells were then pipetted into the glass tubes and dried in a convection oven (Termaks, Bergen, Norway) at 105 °C for 15-17 h and then before weighing were colled in a desiccator. An OD_{600} of 1.0 corresponded to 0.46 g/L (re-check).

Ammonia Assay

Cell samples collected for OD measurement were centrifuged at 12,000xg for 2 min and the supernatant was used for the determination of ammonia at that particular time frame of the fermentation. The samples starting from the C:N ratio experiments were starved of the nitrogen source to produce lipids, to determine the nitrogen-limited phase the Megazyme Rapid Ammonia Assay Kit (Megazyme, Bray, Ireland) was used. The assay is also known as K-AMIAR determines the amount of ammonia that is directly stochiometric to the amount of nicotinamide-adenine dinucleotide phosphate ($NADP^+$). The principle behind the assay as explained in the kit measures the amount of $NADP^+$ formed when 2-oxoglutarate reacts with reduced nicotinamide adenine dinucleotide phosphate (NADPH) and ammonium ions (NH_4^+) in the presence of glutamate dehydrogenase (GIDH), alongside $NADP^+$ there is also formation of L-glutamic acid and water. The NADPH consumption is measured at 340 nm using a Jenway 6405 UV/Visible spectrophotometer (Jenway Limited, Essex, UK) and the reaction is carried out in 1cm cuvettes, reaction time varied between 2-5 min depending on the C:N ratios. The procedure uses three bottles as provided in the kit (link website) the volumes were halved with the final reaction volume of 1.31 mL.

Sugars

The samples collected were centrifuged at 12,000xg for 2 min and then the liquid was transferred to a 2 ml Eppendorf tube and the cell pellet was discarded. The solution was analyzed for carbohydrates (glucose, glycerol, and xylose) using an HPLC (Waters, Milford, MA, USA). The HPLC setup consisted of an Aminex HPX- 87H (BIO-RAD, Hercules, CA, USA) column externally heated at 60 °C (Waters Column Heater Module) with 0.6 ml/min flow rate of 0.005 M sulfuric acid in distilled water as mobile phase a UV detector (Waters 2487), RI detector (Waters 2410), an autosampler and an isocratic solvent pump (Waters 1515).

Lipid Analysis

The samples from the nitrogen limitation experiments were analyzed for fatty acids using Andlid *et al* method of extraction using KOH/ethanol but with a few modifications. An internal standard of 4 mg/mL decanoic acid (Sigma-Aldrich, USA) in toluene was used for the analysis. The sample OD/CDW values were used to measure 25 mg of biomass which was added to 250 µL of internal standard, followed by the addition of 5 mL 2.14 M KOH (prepared in 12% EtOH) and incubation of 2 hours at 70°C. Post incubation, acidification of samples to pH 2 was done by addition of 2.5 mL of 5M HCl. Extraction of lipids was done using heptane in batches of 4+3+3 mL, the mixture was then evaporated under a constant flow of N_2 gas at 40-50°C. Once all the heptane was evaporated, samples were methylated using a mix of 1 mL of 10% acetyl chloride (prepared in methanol) and 1 mL of toluene, followed by incubation at 70°C for 2 hours. Following incubation, samples were extracted in a mixture of 0.4 mL deionized water and 2 mL ether mix of 80:20 petroleum ether/diethyl ether and mixed thoroughly. The upper phase was collected and evaporated under a constant flow of N_2 gas at 40-50°C. the samples were stored in 2 mL heptane for analysis and storage. Before analysis 0.5 mL of samples were diluted in 0.5 mL of heptane in GC vials. The fatty acid methyl esters (FAME) were analyzed using Agilent Technologies GC (USA: GC 7890B), with a flame ionization detector (FID) and an Agilent 122–2362 DB-23 column with 60 m × 250 µm and 0.25 µm film thickness. Helium gas was used as a carrier at a constant flow of 1mL/min. The split injection was set at a 15:1 ratio at 275°C. The method was programmed to have an initial column temperature of 100°C followed by a 4°C/min increase until a temperature of 250°C, which was held for 4 min before decreasing down to 100°C. The fatty acid content of the samples was determined by back-calculation of the internal standard concentration.

OptFlux Calculations

Table 1: Input constraints (consumption) and output (production) values for C:N 100 nitrogen limitation condition

Consumption			Production		
Metabolite Id	Metabolite Name	Value	Metabolite Id	Metabolite Name	Value
M_nh4_e	Ammonium	0.12	M_tag_c	Triacyglycerol (tripalmi...	0.20759
M_pi_e	Phosphate	0.09643	M_h_e	H+ (extracellular)	0.35772
M_so4_e	Sulphate (extracellular)	0.003	M_h2o_e	water	8.76421
M_o2_e	O2 (extracellular)	3.5949	M_co2_e	Carbon dioxide	8.0173
M_glc_e	Glucose	3.34	M_cell_mass_c	Cell mass	0.01964

The input values as seen in Table 1 were calculated based on the obtained glucose and ammonium salt molar consumption per cell dry weight (C-mol/g CDW; N-mol/g CDW) at the end of fermentation. The input values for hexose exchange i.e. glucose uptake and $NH4^+$ uptake follow the cell mass equation from the Castañeda *et al*. metabolic model resulting in cell mass, triglycerides, CO2, and water production. Experimentally obtained values of cell density (OD values) were used to plot a log(X-Xo) with respect to time to obtain the growth rate μ in h^{-1}. The glucose uptake rate was calculated using the formula $r_s = Y_{XS} * \mu$, the Yxs was calculated by plotting the glucose consumption measured in m.mol/L and the CDW in the exponential phase of the fermentation. A similar procedure was repeated for ammonia consumption and the obtained values were input in the OptFlux software. The resulting values of cell mas are in C-mol/ g CDW, using the C-mol formula used for *R. Toruloides* by Castañeda et al. which results in 73.09 C-m.mol/g.h cell mass and the molecular weight is based on the empirical formula $CH_{1.76}O_{0.58}N_{0.16}$ which is 25.31 g/C-mol. The predicted growth rates were then calculated using the simulated values and the fluxes were converted into yields. The simulated yields were then compared with the experimental yields and comments on the model's prediction were made.

Flow cytometry

Flow cytometry for fed-batch samples was done using a BD Accuri C6 flow cytometer with a BD CSampler autosampler (Becton–Dickinson, NJ, US). The wavelength of the laser was 488 nm, four filters with the following emissions were used: Filter 1: 533/30 bandpass filter (FL1 channel), Filter 2: 585/40 bandpass filter (FL2 channel), Filter 3: 675/25 bandpass filter (FL3 channel), Filter 3: 670LP long-pass filter (FL4 channel). The instruments detection threshold was set greater than equal to 80,000 on the FL1-H channel and the events collection threshold was set at 100,000 events/sample. A flow rate of 14µl/min was used and the core size was set to 10µm. The samples for flow cytometry before injection were diluted to an OD of 0.4 and after each sample, the machine was injected with MilliQ water for 2 minutes at a flow rate of 66 µl/min and a core size of 22µm to minimize carryover of samples. The results obtained were analyzed by a software called FlowJo (v10.7.1 ; Treestar, Inc., San

Carlos, CA). All channels were analyzed by height (FSC-H, FL1-H, etc.) and geometric mean was used to quantify the signal on the following channels: FSC-H, SSC-H, FL1-G, FL2-H, FL3-H, FL4-H. In this thesis, we will be more focused on FSC-H (forward scatter), SSC-H (side scatter), and FL-1 (fluorescence in channel 1) (Osiro *et al.*, 2019).

RESULTS & DISCUSSION

Shake flask fermentation for culture condition determination

A) Assessing growth on different carbon sources

The experimental work started with shake flask cultivations of *R. toruloides* on glucose, glycerol, and xylose as substrates and at a temperature of 30°C and pH of 5.5. The microorganism consumes all of the glucose and xylose within 72 hours, but for glycerol, the lag phase was considerably longer and growth did not occur until after 50 h when a significant change in OD was seen between 54 to 72 (fig 3). The highest consumption rate was found for glucose, followed by xylose and lastly glycerol as seen in Table 2. The concentration of carbon source used in this shake flask experiment was 20 g/L and *R. toruloides* is known to tolerate up to 80 g/L of glucose but shows a substantial amount of substrate inhibition at 120 g/L (Sitepu *et al*.,2014).

Table 2: Biomass yield and specific growth rate values for glucose and xylose carbohydrate source

Experiment	Y_{SX}(g/g)	μ(h^{-1})
Glucose	0.60	0.16
Xylose	0.78	0.15

The obtained yields, Ysx, (g dwt biomass produced/g substrate consumed) were 0.6 for glucose, and 0.78 for xylose (Table 2). The Ysx for glycerol was not included as no significant growth was observed until 54 hours of fermentation as seen in fig 3, and one of the glycerol duplicates showed no growth. The specific growth rates based on the CDW and fermentation time were 0.16 h^{-1} for glucose, 0.12 h^{-1} for glycerol, and 0.15 h^{-1} for xylose (raw data in Appendix I, Table A:1,4). *R. toruloides* has been previously reported to consume hexoses and pentoses alike with no preference for a specific sugar (Sitepu *et al*.,2014; Bommareddy *et al*.2015). The strain used in this research reflected similar results, in the sense that it consumed both glucose and xylose with very closely related values of Ysx and μ, but glucose was selected for the rest of the experiments to allow comparison with pre-existing literature.

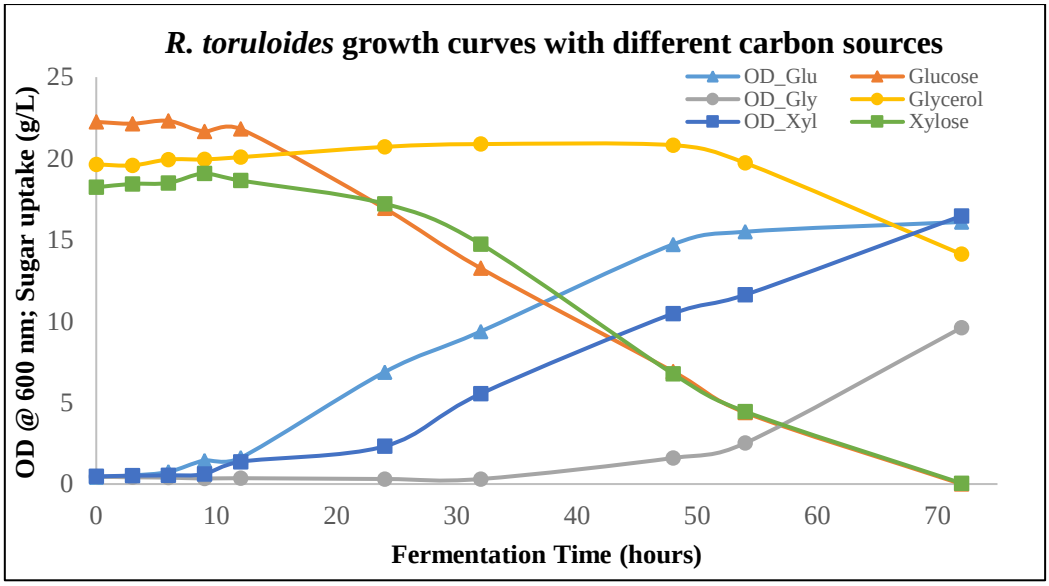

Figure 3: *R. toruloides* growth curves for OD_{600} and sugar uptake at different carbohydrate sources (glucose, glycerol, and xylose).

B) Temperature effects

The carbohydrate source experiment was followed by characterization of temperature experiment, the 30°C data was taken from the previous experiment, and experiments on temperatures 27, 33, and 36°C were carried out. Obtained experimental results for Y_{SX} and μ as seen in Table 3 indicated highest Ysx at 27°C and highest μ at 33°C. As seen in fig 4, the highest OD values and volumetric glucose consumption rates were found for cells growing at 27°C followed by 33°C, and the lowest OD was found at 36°C.

Table 3: Biomass yield and specific growth rate values at different temperatures (raw data data in appendix I, Table A:2, 4)

Experiment	Ysx(g/g)	μ(h^{-1})
36°C	0.45	0.20
33°C	0.49	0.24
30°C	0.60	0.16
27°C	0.62	0.19

The yeast shows growth at all temperatures, although for this strain 27°C was preferable previous research by Li et al., reported optimal lipid production at 30°C so for ease of further experimentation 30°C was chosen as the cultivation temperature. The temperature experiments resulted in different carotenoid pigmentation as seen in fig 5. The pink pigmentation also appeared at different fermentation times. Carotenoids according to Linus Paul Institute can be defined as yellow, orange, and red pigments synthesized by plants and some microorganisms. This variance is assumed to be indirectly related to

temperature stress, and brighter pigmentation could be an indication of the yeasts' well-being. The effect of temperature on the growth of *Rhodotorula mucilaginosa* was previously reported to show maximal growth rates and carotenoid yields at 30°C which was reflected in this experiment as well with brighter pigmentation in the 27-30°C range (Naghavi,2014).

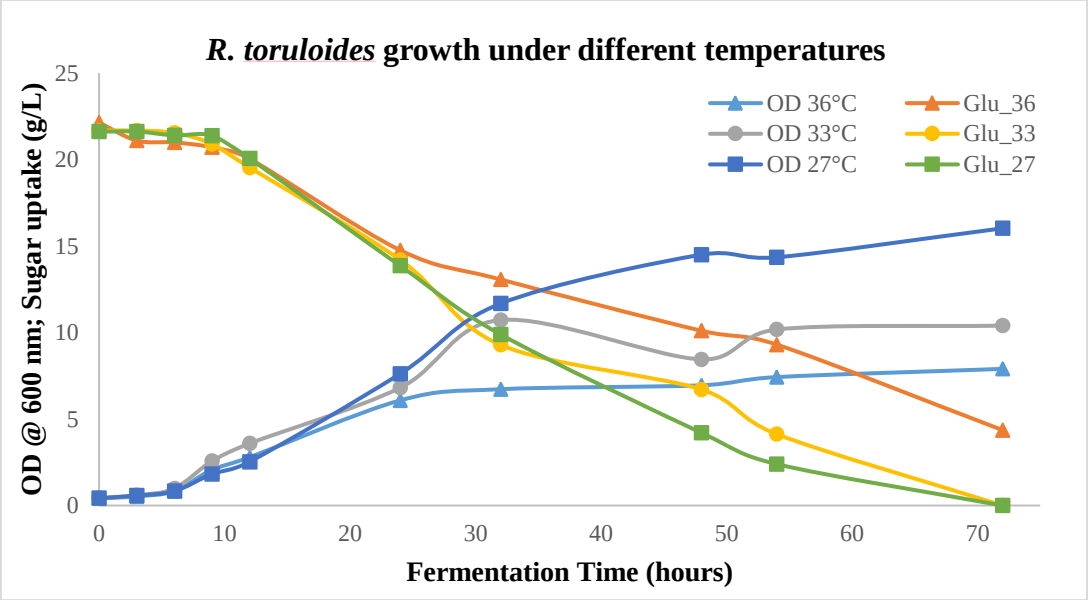

Fig 4: *R. toruloides* growth curves for OD_{600} and glucose uptake at different temperatures (36,33 and 27°C)

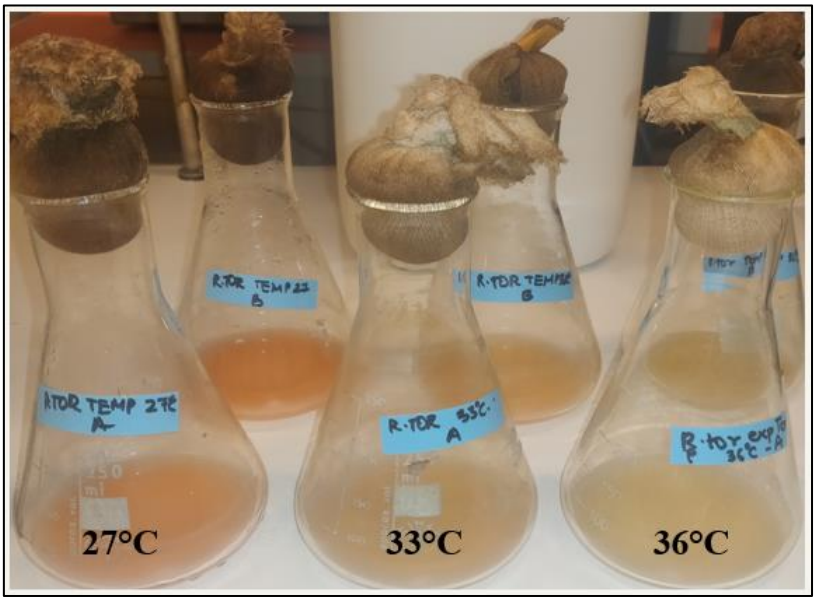

Fig 5: *R. toruloides* cells after 72 hours of growth at different temperatures showing difference in pigmentation

C) pH effects

The last set of characterization experiments was focused on pH, the chosen range was between 4.0 to 6.5 as previous research by Johnson *et al.* suggests that *R.toruloides* showed a higher lipid accumulation at pHs between 4.0-5.0, and research by Naghavi suggested a pH of 5.0 due to higher carotenoid yields and growth rates (Johnson *et al*,1992; Naghavi, 2014). The pH experiments for this strain resulted in the highest Ysx at pH of 6.5 and highest μ at pH of 4.5 (Table 4).

Table 4: Biomass yield and specific growth rate values at different pHs′(raw data in appendix I, Table A:3, 4)

Experiment	Ysx (g/g)	μ (h^{-1})
6.5 pH	0.83	0.18
5.5 pH	0.60	0.16
4.5 pH	0.67	0.21
4.0 pH	0.59	0.12

The glucose consumption and OD trends are shown infig 6, the highest OD and glucose consumption is seen at pH 6.5 followed by pH 4.5 and least for pH 4.0. The pH was measured throughout fermentation. A drop in pH was noted only for the first 24 hours, which could be indicative of the yfigeasts adjusting to the cultivation environment. Similar to the temperature experiments, carotenoid intensity changes with stress and the optimal conditions results in higher colour intensity, OD, and growth rates (fig 7). The yeast exhibits excellent resilience at various pH conditions but to allow comparison of experimental data with pre-existing literature pH of 5.5 was selected.

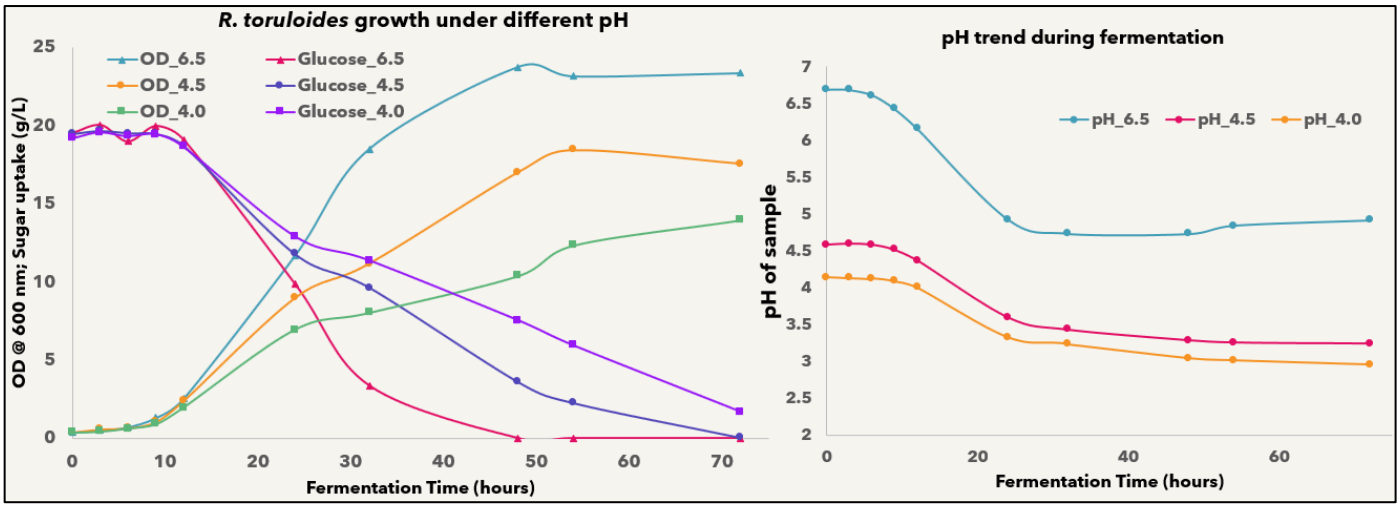

Fig 6: *R. toruloides* growth curves for OD_{600} and glucose uptake at different pH (L), pH trend during shake flask fermentation (R).

Fig 7: Centrifuged *R.toruloides* cells after 72 hours growth at varying pH showing variance in pigmentation.

Shake flask fermentation for lipid production

As mentioned in the background nitrogen limitation in the presence of enough carbon is what induces lipid accumulation (Papanikolaou and Aggelis, 2001). Therefore a higher C:N ratio would likely give a higher lipid production. To further study how lipid accumulation would take place in *R. toruloides* BOT A-2 strain, various carbon to nitrogen (C:N) molar ratios were tested. The nitrogen limitation experiments used the culture conditions from the characterization experiments i.e. glucose as the carbon source, cultivation temperature of 30°C, and a pH of 5.5. The C:N molar ratios of 20, 40, 80, and 100 were tried for this strain. The C:N molar ratios were selected based on the work by Braunwald *et al*. on *Rhodotorula glutinis*, where C:N molar ratios of 20-120 were reviewed (Braunwald *et al.*,2013). The concentration of glucose was maintained at 20 g/L while the nitrogen concentration was varied as per experimental requirement.

The experiment resulted in glucose and OD trends as seen in fig 8, the highest OD was recorded for C:N 100 followed by C:N 20, 80, and 40 (raw data in appendix II, Table B:1,2). All the C:N ratios show complete glucose consumption after 72 hours of fermentation. The ammonia (nitrogen source) concentration in all the ratios varies greatly, signifying the reducing amount of in accordance to C:N 20 to 100 molar ratios. The C:N 20 ratio does not show complete consumption of ammonia, while all others show exhaustion of ammonia after 24 hours of fermentation. Another notable trend in the graphs is the flat-lining in OD as a result of nitrogen and glucose exhaustion, which is only seen in C:N ratios above 40. The above phenomenon is reflective of the yeasts sensitivity to environmental stresses (exhaustion of nutrients).

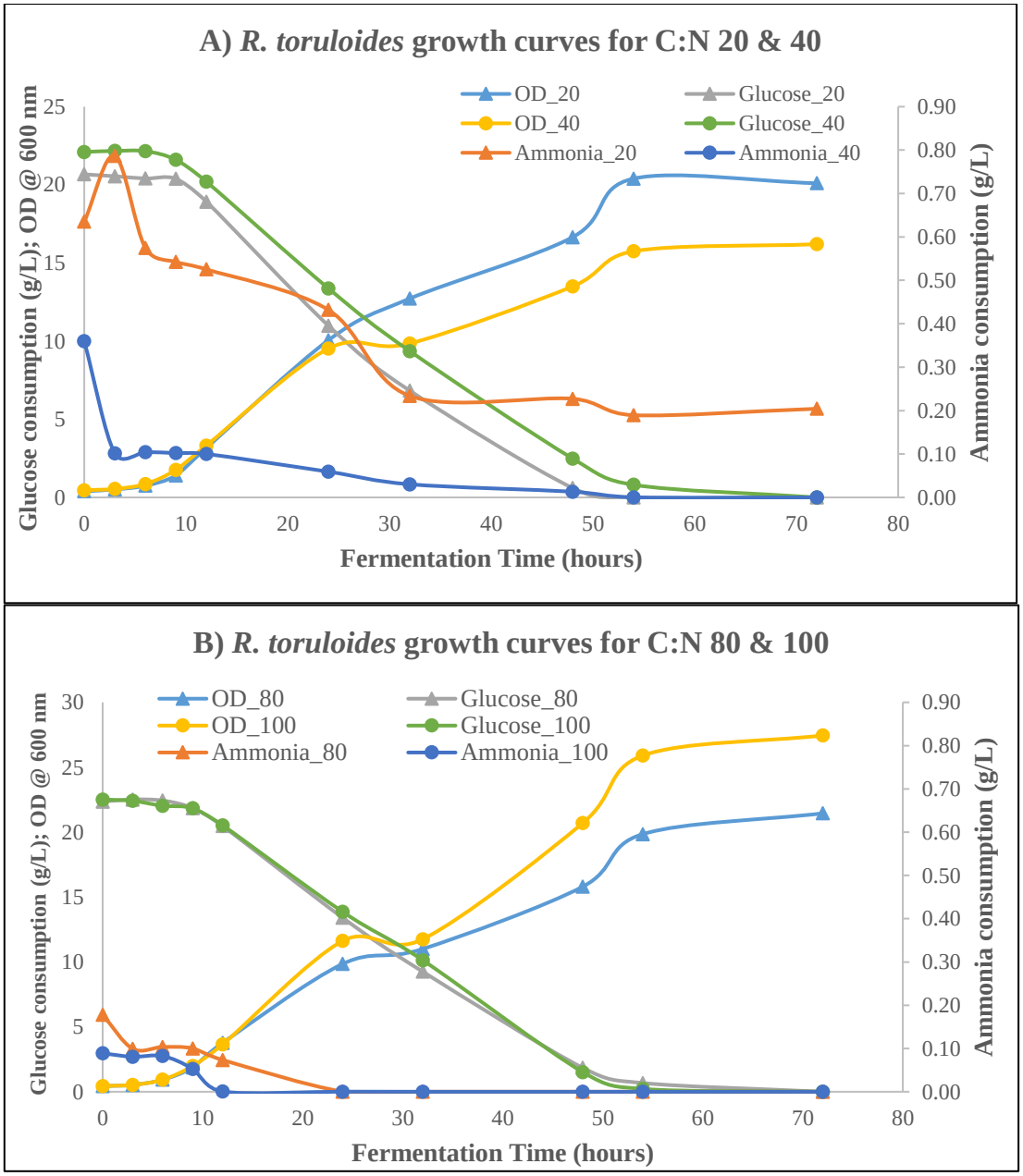

Fig 8: *R. toruloides* growth curves for OD, glucose and ammonia consumption at different C:N ratios A) at C:N 20 and 40; B) at C:N 80 and 100

Table 5: Biomass yield, ammonia yield and specific growth rate values at different C:N ratios (raw data in appendix II, Table B:3)

Experiment	Y_{SX} (g/g)	Y_{SN} (g/g)	μ (h^{-1})
C:N 20	0.62	0.11	0.24
C:N 40	0.58	0.07	0.20
C:N 80	0.50	0.05	0.22
C:N 100	0.50	0.03	0.22

The difference in nitrogen trends can be further correlated to the Y_{SN} values which decline from C:N 20 to 100 (Table 5). The highest Y_{SX} and μ are observed for C:N 20 which can be attested to the absence of nitrogen limitation, which allows the cells to grow well. The specific growth rates calculated from the measured OD in the exponential phase before nitrogen limitation set in, based on that it can be said that the growth rates in that exponential phase are independent of nitrogen limitation. The OD, glucose, and ammonia concentration analyses were accompanied by lipid analysis for the nitrogen limitation experiments. Fatty acid analyses were made using the GC and the total lipid content can be visualized in fig 9. The lipid accumulation was found to be 19%, 22%, and 36% at C:N ratios of 40,80, and 100, respectively (raw data appendix III, table C.1). The C:N 20 showed no accumulation, in line with the fact that there was no nitrogen limitation condition induced during this experiment. The lipid accumulation varies amongst the different C:N ratios as higher the carbon to nitrogen ratio at the beginning of the fermentation, the higher is the amount of Acetyl-CoA being channelled to the TAG synthesis pathway (Braunwald et al.,2013). Braunwald et al.,2013 reported accumulation for C:N 20, while our research did not; they also reported the highest accumulation at C:N 70 ratio with an initial glucose concentration of 57 g/L, and slightly lesser accumulation for C:N 120.

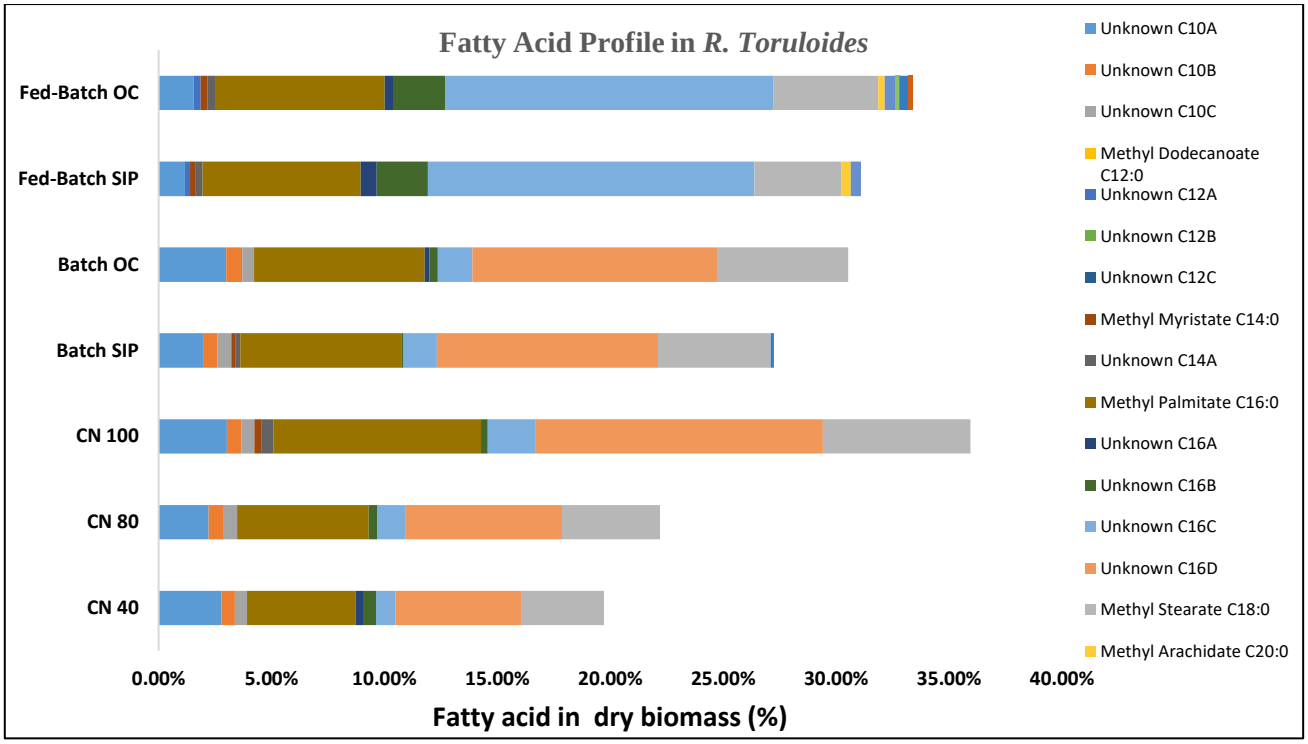

Fig 9: *R. toruloides* fatty acid profile for nitrogen limitation shake flask and batch bioreactor experiments

The pink colour of the cells due to the presence of carotenoids was similar in intensity at the end of fermentation i.e. 72 hours (fig 10), but the cells turned pink at different time points - possibly caused by the stress from low ammonium concentration. An inverse relation between carotenoid and lipid production has been previously reported (Somashekar and Joseph, 2000). The lipid profile shows the presence of fatty acids with an even number of carbon atoms in the backbone such as palmitic acid (C16:0), stearic acid (C 18:0), oleic acid (C18:1), linoleic acid (C 18:2), and traces of lauric acid (C12:0) and myristic acid (C14:0) (Shen et al., 2017). The internal standard used was decanoic acid (C:10). The profile shows the highest percentage of C:16 in the C:N 100 shake flask and lower percentages in lower C:N ratios. It has been previously reported that as the C:N ratios are increased the unsaturated fatty acids start to dominate and the results of this study follow the trend (Mondala et al.,2011).

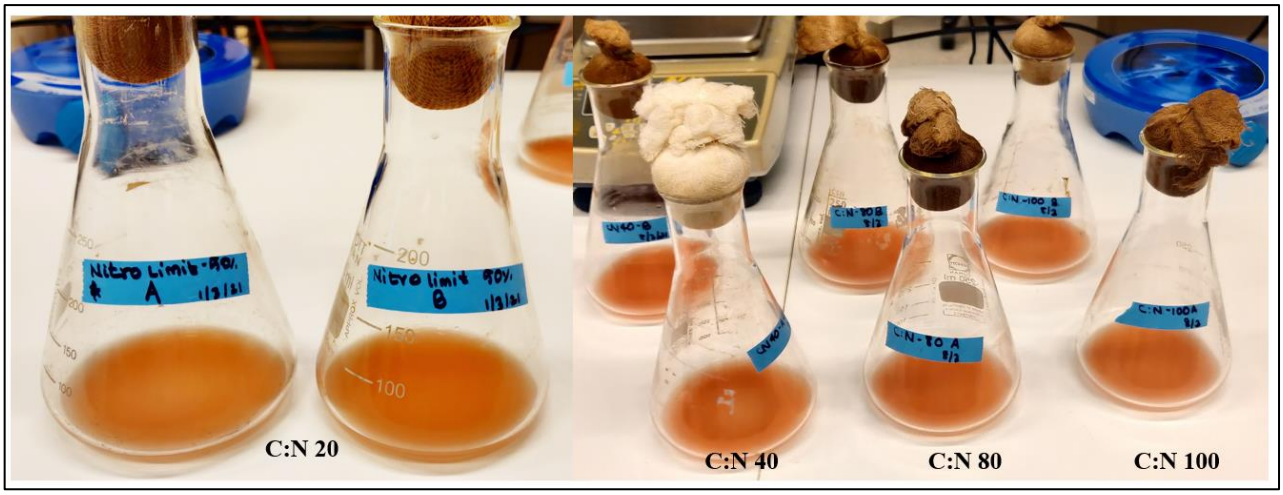

Fig 10: Carotenoid pigmentation in various C:N molar ratios after 72 hours of fermentation

Bioreactor fermentations

The nitrogen limitation shake flask experiments gave us an insight regarding which C:N ratios accumulate a higher amount of lipids, following the shake flask the experiments were scaled up to bioreactors. The reasoning for the scale-up was to allow better control of pH and try different feeding strategies (batch and fed-batch), and check how much lipid the yeasts can accumulate. The bioreactor experiments were done using two feeding strategies: (i) batch mode – the initial glucose load was increased to 50 g/L and the fermentation time was 72 hours; (ii) fed-batch – the initial glucose concentration was maintained at 20 g/L, a feed rate of 0.7 g/h of 400 g/l glucose stock solution was initiated after 24 hours (expecting nitrogen exhaustion at this point). The bioreactors used can be visualized in fig 11 and will be referred to as: (i) **Sterilization in place (SIP)**, and (ii) **Old control (OC) reactors**.

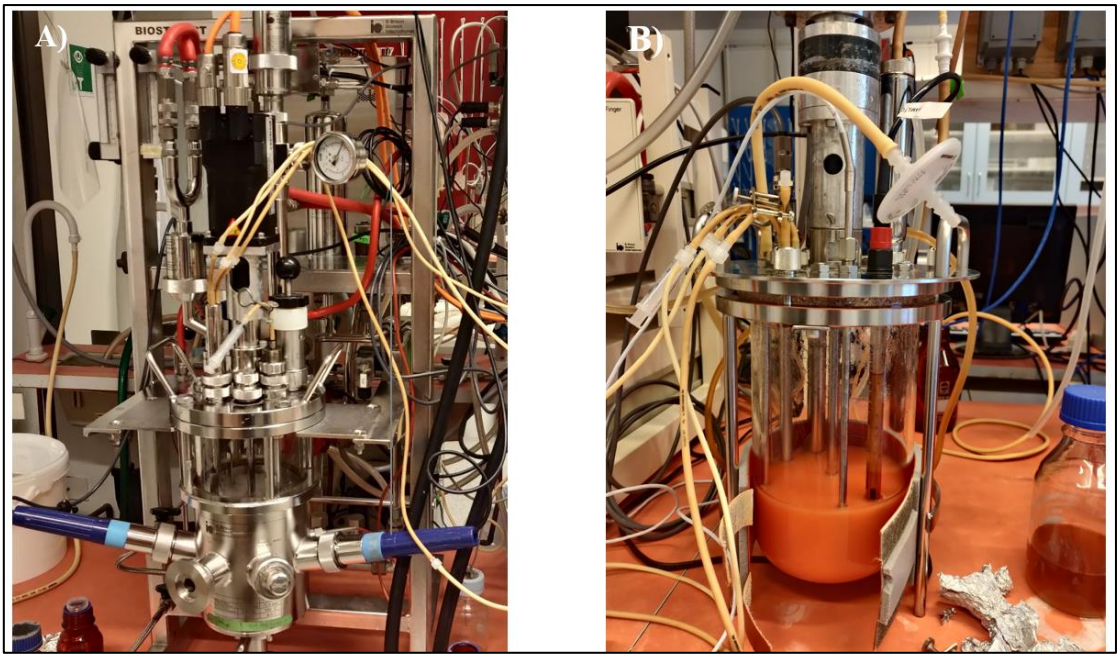

Fig 11: The two bioreactors for batch fermentation. A) The SIP setup B) The OC setup

I) Batch Bioreactor fermentations

The batch experiments had the following process parameters: temperature at 30°C, stirrer speed of 400 rpm, pH of 5.5, initial substrate concentration of 50 g/L, and C:N ratio of 80. The C:N ratio 80 was selected based on the previous shake flask results, as the cells were more stressed at C:N 100 due to lower nitrogen concentration despite showing higher lipid accumulation. A concentration of 50 g/L glucose was used, as no inhibitory effect was expected based on the research done by Li *et al.* Higher sugar concentrations gave a prolonged fermentation period, and as seen in fig 12. The glucose was completely consumed after 78 hours for the SIP reactor, whereas the glucose was not consumed until after 120 hours for the OC reactor indicating the possibility of longer fermentation. The reason for the difference in the glucose consumption pattern could be different oxygen transfer conditions. The number of impellers (two Rushton turbines in SIP while only 1 in OC) and the number of baffles (4 in SIP and only 1 in OC) differed in the two reactors.

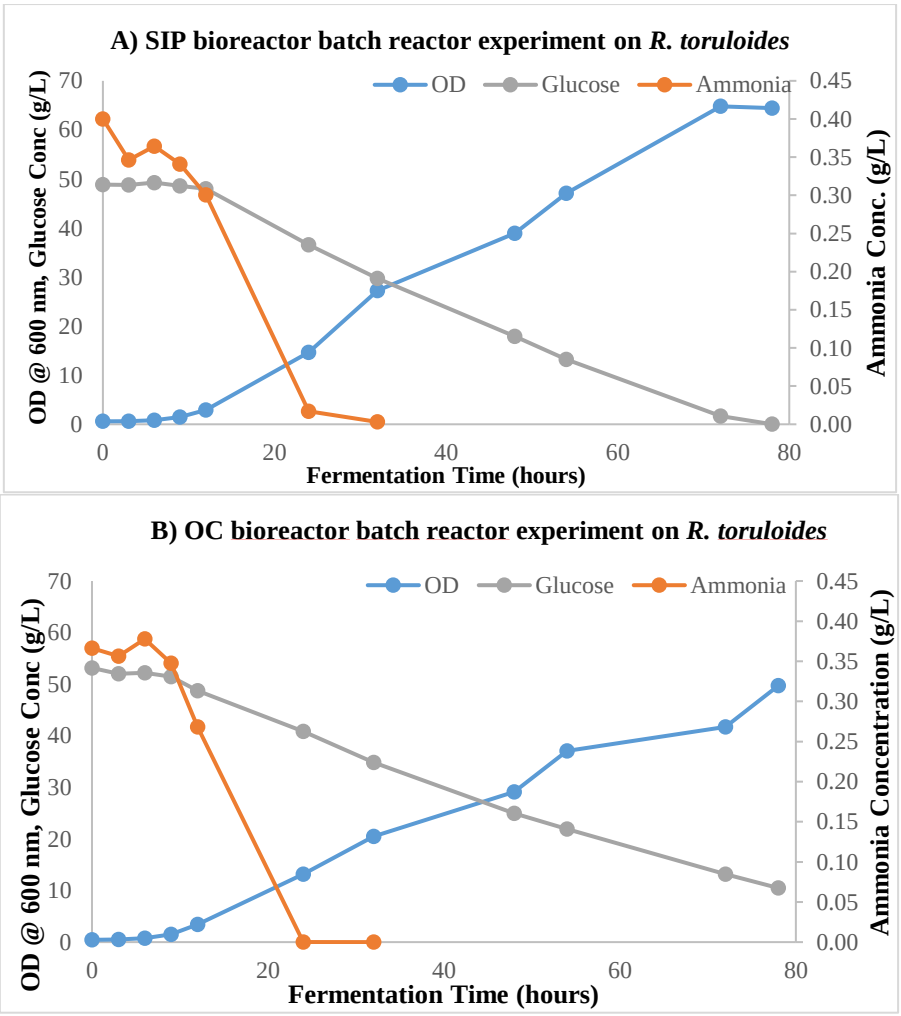

Fig 12: *R. toruloides* growth curves for OD, glucose and ammonia consumption during batch cultivation in the two bioreactors A) SIP, Sterilization in place bioreactor; B) OC, Old Controls bioreactor (raw data appendix IV, Table D.3)

Table 6: Biomass yield, ammonia yield, and specific growth rate values for batch experiments

Experiment	Y_{SX} (g/g)	Y_{SN} (g/g)	μ (h^{-1})
SIP	0.455	0.062	0.17
OC	0.405	0.049	0.22

As seen in Table 6, the Y_{SX} is higher for the SIP reactor whereas the μ is higher for the OC reactor (raw data appendix IV, Table D.1). The fatty acid profiles as seen in fig 9 (nitrogen limitation shake-flask results section) show ~27% of lipid accumulation in the SIP reactor and ~31% of lipid accumulation in the OC reactor. The lipid profile shows the dominance of unsaturated C:16 fatty acid composition, which was also observed in the shake flask experiments (C:N 80 was observed to have a 22% biomass to lipid conversion). The lipid profile shows a 10% increase in accumulation, which

could be credited to higher initial glucose concentration (Yaegashi *et al.*,2017). More lipid accumulation was assumed to affect cell size to further investigate this, cell counting with respect to cell dry weight (CDW) was carried out at certain time frames as seen in fig 13, which suggested that the cell number increased exponentially throughout despite nitrogen limitation. The reason for that could be due to the presence of organic nitrogen in the form of amino acids in the cultivation media of the inoculum, which allowed the cells to grow in the later stages when the volume of the amino acids due to nitrogen limitation would have declined to critical levels.

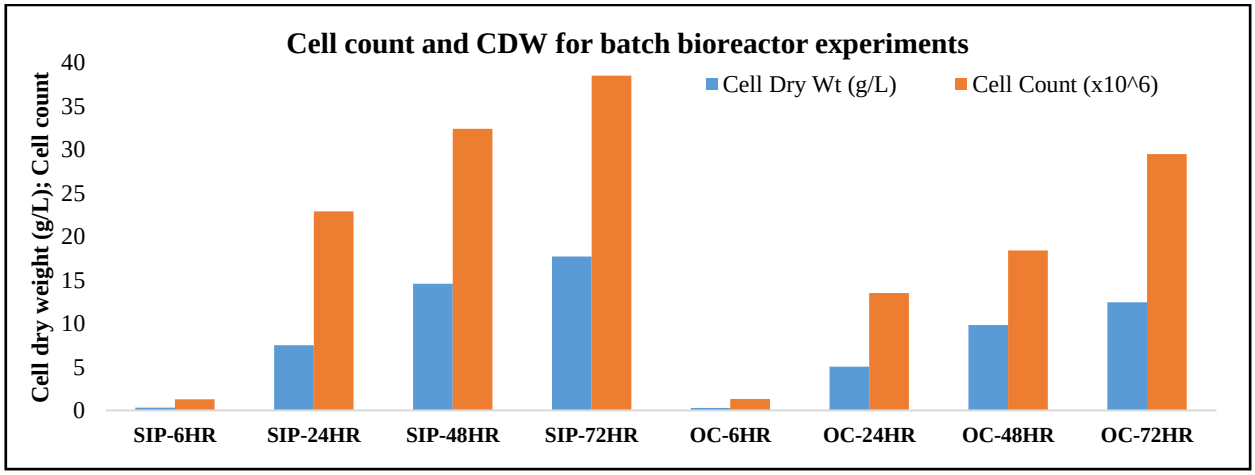

Fig 13: Cell count and CDW in g/L comparison at different fermentation time points (raw data appendix IV, Table D.2)

II) Fed-batch bioreactor fermentations

The batch experiments showed the possibility of longer fermentation periods, which were applied in the fed-batch experiments. The OC reactor was given the same amount of baffles and turbines as the SIP reactor and the process parameters were maintained at a temperature of 30°C, stirrer speed of 500 rpm (to avoid foaming), pH of 5.5, initial substrate concentration of 20 g/L, and C:N ratio of 80. The feed was started after exhaustion of ammonia at 24 hours with a feed rate of 0.7 g of glucose/hour which was equated to 2% of pump capacity.

Table 7: Biomass yield, ammonia yield and specific growth rate values for fed-batch SIP and OC reactor (raw data Appendix V, table E.2)

Experiment	Y_{SX} (g/g)	Y_{SN} (g/g)	μ (h^{-1})
SIP	0.540	0.182	0.19
OC	0.478	0.186	0.16

As seen in fig 14, the OD for both the reactors follows the same trend as the batch experiments for the first 24 hours of fermentation. The SIP reactor OD trend shows a plateau at 72-hour mark, which could

be due to a miscalculation of OD. The glucose trend in both reactors shows accumulation after 96 hours of feeding, suggesting that we are pumping glucose faster than the cells can consume it. The ammonia consumption curve indicates exhaustion after 24 hours in both reactors. The growth rate in the batch phase (0-24 hours) was calculated to be ~0.2 h^{-1} for both the reactors (Table 7). The Ysx was higher for the SIP reactor as compared to the OC reactor. The high Y_{SN} values are due to higher amount of organic nitrogen (amino acids) in the inoculum.

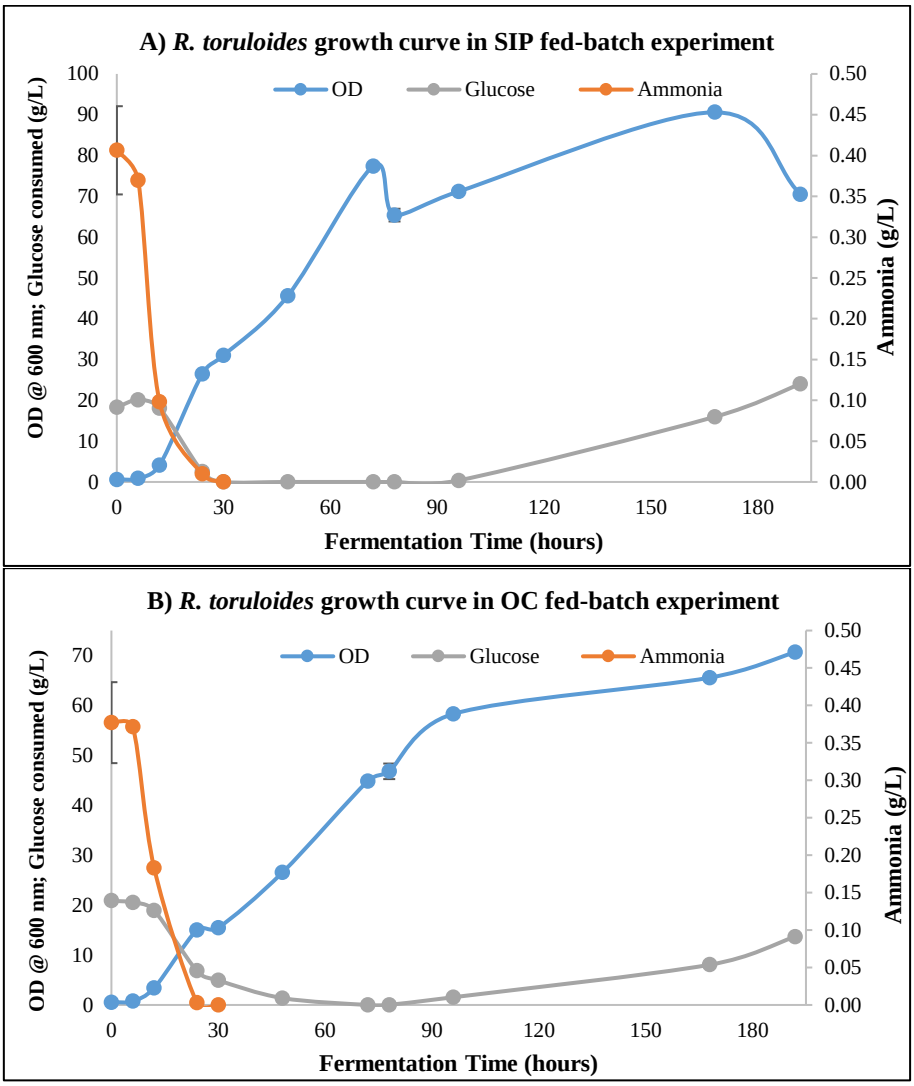

Fig 14: *R. toruloides* growth curves for OD, glucose and ammonia consumption in different fed-batch bioreactors A) SIP, Sterilization in place bioreactor; B) OC, Old Controls bioreactor (raw data Appendix V, table E.1)

The feed was to be continued until a drop CO_2 levels was noted indicating that cells have reached their glucose consumption limit, but the levels stayed at 0.6% CO_2 in the atmosphere. The fermentation was stopped at 192 hours as centrifugation of samples was becoming increasingly difficult, it was seen that the cells had burst and released lipid into the fermentation medium as seen in fig 15, the centrifuged

sample shows the presence of lipids in the culture media alongside live cells and cell debris from dead cells. To further investigate, the cells were viewed under the microscope and cells at different growth phases, cell debris, and swollen cells could be visualized. The cells were assumed to gave reached their maximal lipid accumulation phase and hence burst, which further led to a change in the density of the sample making it difficult to centrifuge. The fatty acid profiles as seen in fig 9 (nitrogen limitation shake-flask results section) show ~32% of lipid accumulation in the SIP reactor and ~34% of lipid accumulation in the OC reactor. In the fed-batch experiments due to some cells bursting, lipid was also present in the reaction media and therefore the amount of lipids analyzed are much lower than the actual lipids produced during the experiment. The lipid accumulation here could also indicate that starting at higher glucose loading (50 g/L in batch) could have led to inhibition of the TAG synthesis pathways (Fei *et al.*, 2016). So, it would be beneficial to have fed-batch cultivations to obtain higher lipid accumulation which occurs at later stages of fermentation.

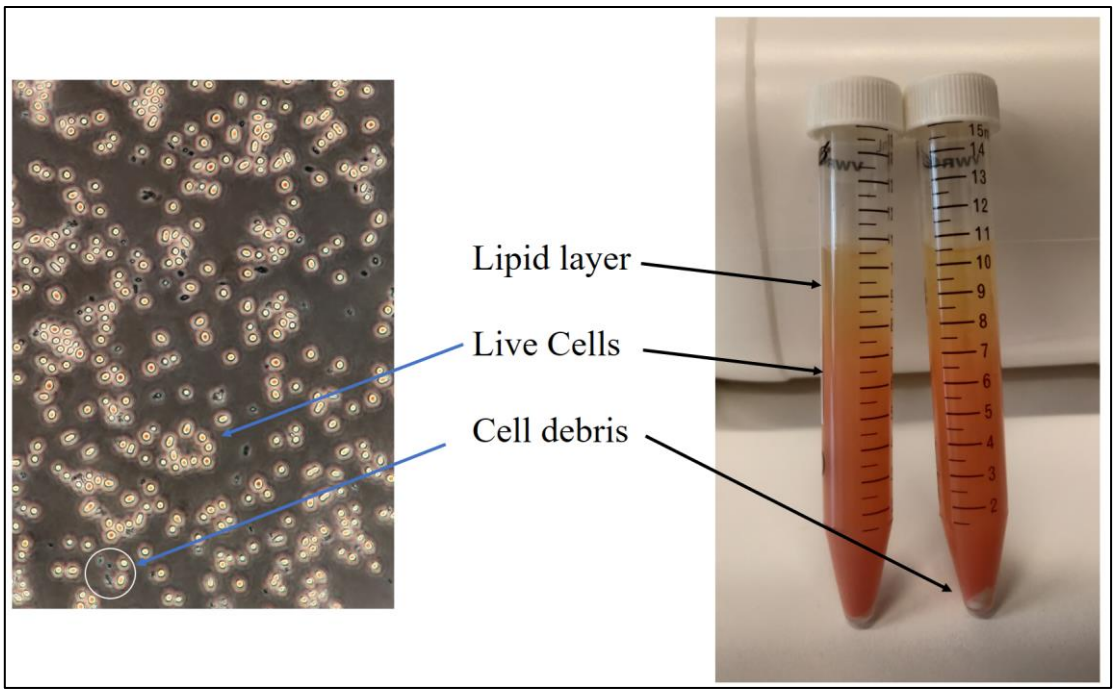

Fig 15: *R.toruloides* cell under the microscope after 192 hours of fermentation and centrifuged samples showing cell density gradient

To further study the effect of the size of the microorganism on lipid accumulation flow cytometry was carried out and the results as shown in fig 16. The plots for SIP and OC reactor showed similar trends so only SIP plot was included in this section, the OC plot can be seen in appendix VIII fig G.1. In fig 16.A, in the batch phase (0-24H), there appear to be two populations of cells, and as the feeding phase is reached the geometric mean plots start leaning towards the right and the narrowing of the peak

represents increase in cell size. The 16.B plot represents the fluorescence from filter-1 was used to determine the scatter of carotenoids as they absorb between 440-467 nm (Sen Gupta & Ghosh,2013). From the plot, it can be assumed that the two populations are probably cells with carotenoids and cells without them, and after 12H most cells show pink colouration. The 16.C plot, which represents side scatter is indicative of granularity starts leaning rightwards after 96 hours until 192 hours, which is indicative of accumulation of lipid in the fermentation media due to the cells bursting (Leif, 1986).

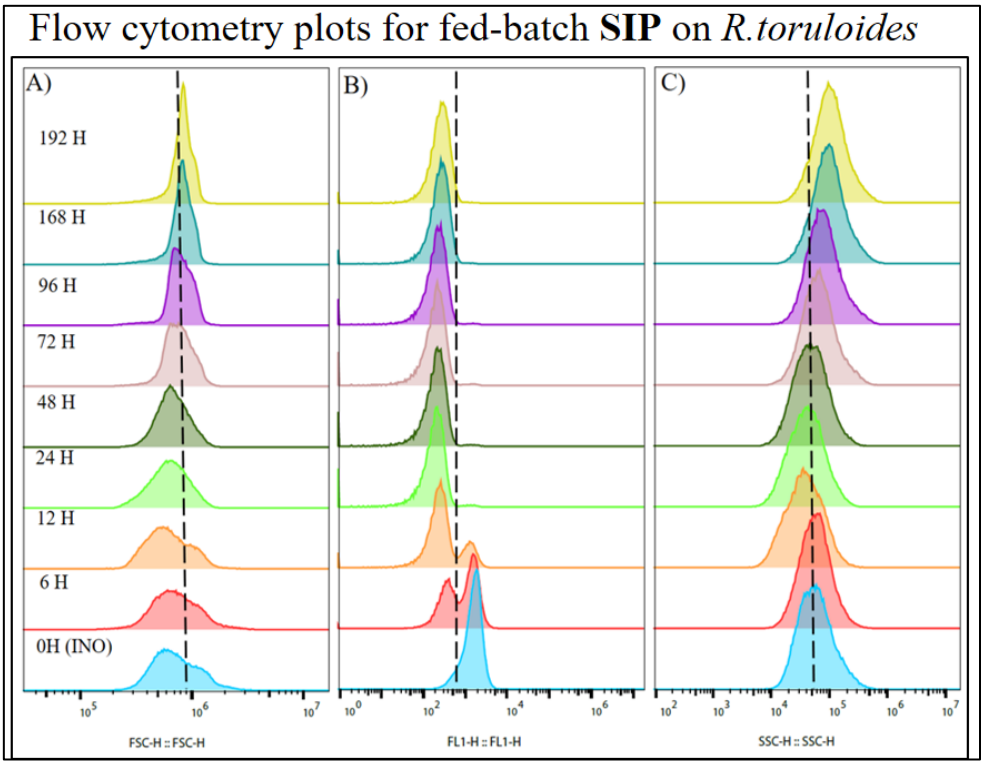

Fig 16: Flow cytometry geometric mean results for the whole duration of SIP fed-batch fermentation. A) Forward scatter SIP fermentation; B) Scatter plots for filter FL1 for SIP; C) Side scatter for SIP

Optflux simulations

The last part of the thesis included comparing experimental data with simulated data from Castañeda *et al*. metabolic model simulated in OptFlux. As mentioned in the introduction OptFlux using flux balance analysis to predict specific growth rates and lipid production rate. The glucose and nitrogen uptake rates were input into the software and the resulting biomass and lipid production was simulated as seen in table 8 (raw data appendix VII, table F.1,2).

Table 8: Experimental and simulated biomass and lipid yield values

Experiment	Experimental Y_{SX} (g/g)	Y_{SX} Simulated (g/g)	Experimental Y_{STAG} (g/g)	Y_{STAG} simulated (g/g)
CN:20	0.43	0.31	0.00	0.36
CN:40	0.25	0.18	0.066	0.45
CN:80	0.28	0.13	0.078	0.49
CN:100	0.30	0.07	0.154	0.53
Batch SIP	0.49	0.18	0.165	0.45
Batch OC	0.21	0.11	0.120	0.50
Fed batch SIP	0.41	0.15	0.171	0.47
Fed batch OC	0.35	0.10	0.182	0.51

The Y_{SX} experimental and simulated values are comparable for lower C:N molar ratios but become increasingly incomparable for higher ratios (C:N 100). The model assumes too much stress caused due to higher nitrogen limitation and predicts much lesser biomass than expected. For the reactor experiments, the simulated values show similar Y_{SX} values as the C:N 80 molar ratio was maintained, but the experimental values differ due to change in reactor parameters which are out of the model's domain. The Y_{STAG} values for experimental and simulated values are not comparable at all, the model shows lipid accumulation at C:N 20 molar ratio while the experimental conditions showed lipid accumulation as nitrogen limiting condition was never reached. The model seems to clearly overestimate the lipid production values. The deviation between experimental results and simulations could partly be due to the fact that the uptake glucose and nitrogen rates were taken from the exponential phase rather than the nitrogen limitation phase. The model further does not account for more than one nitrogen source, it does not account for the additional amino acids which resulted in higher biomass yields in this research. The Castañeda et al. model is not sufficiently complete or complex enough to accurately predict lipid accumulation under the conditions studied.

CONCLUSION

In this work, I have examined growth and lipid production of the wildtype of the yeast *Rhodosporidium toruloides* BOT A-2. The main findings can be summarized below. The characterization experiments were done for different carbohydrate sources, temperatures, and pHs'. The yeasts can grow on all carbohydrate sources namely glucose, glycerol, and xylose; and shows the longest lag phase for glycerol. The yeast showed highest biomass yield for xylose. For ease of comparison of data with pre-existing literature, glucose was chosen as the preferred carbohydrate source. The yeasts are capable of growing in the 27-36°C temperature range, and show variation in carotenoid pigmentation in response to environmental stress. The highest biomass yield for this strain was reported at 27°C. For ease of comparison of data with pre-existing literature 30°C was chosen. The yeasts showed resilience at pHs' of 4.0, 4.5, 5.5, and 6.5 range, the variance in carotenoid pigmentation was also observed here. The highest biomass yield for this strain was reported for pH 6.5. For ease of comparison of data with pre-existing literature pH of 5.5 was chosen. After the characterization experiments, lipid accumulation was studied at C:N molar ratios of 20,40,80, and 100. The highest accumulation of ~36% was reported for C:N 100 molar ratio, but for further bioreactor experiments C:N 80 was selected to reduce the stress caused due to nitrogen limitation. The bioreactor experiments resulted in highest lipid accumulation in fed-batch strategy as longer fermentation periods were allowed. The fed-batch flow cytometry plots also showed an increase in cell size and presence of carotenoids after 24 hours of fermentation. The final stage of research included OptFlux simulation, the Optflux model designed by Castañeda *et al.* was found to overpredict the lipid accumulation yields.

Suggested further work

Rhodosporidium toruloides BOT A-2 shows a preference for cultivation temperature of 27°C and xylose as a carbohydrate source, this could be further explored. Further research for reduction of the glycerol lag phase would also be beneficial as glycerol is a more industrially viable carbohydrate source. The effect of temperature and pH on carotenoid production should be studied to better understand the lipid accumulation, as research suggests a correlation between the two. For fed-batch bioreactor experiment, it would be beneficial to maintain the feed-rate of 0.7 g/h until 48 hours and then reduce the fed-rate to avoid the accumulation of glucose and reduction of stirrer rate from 500 rpm, as the high aeration led to the bursting of cells and loss of lipids to the fermentation media in this research.

REFERENCES

Ageitos, J. M., Vallejo, J. A., Veiga-Crespo, P., & Villa, T. G. (2011). Oily yeasts as oleaginous cell factories. Applied Microbiology and Biotechnology, 90(4), 1219–1227. https://doi.org/10.1007/s00253-011-3200-z

Andlid, T., Larsson, C., Liljenberg, C., Marison, I., & Gustafsson, L. (1995). Enthalpy content as a function of lipid accumulation in *Rhodotorula glutinis*. Applied Microbiology and Biotechnology, 42(6), 818–825. https://doi.org/10.1007/bf00191175

Blazeck, J., Hill, A., Liu, L., Knight, R., Miller, J., Pan, A., Otoupal, P., & Alper, H. S. (2014). Harnessing *Yarrowia lipolytica* lipogenesis to create a platform for lipid and biofuel production. Nature Communications, 5(1). https://doi.org/10.1038/ncomms4131

Bommareddy, R.R., Sabra, W., Maheshwari, G. et al. (2015). Metabolic network analysis and experimental study of lipid production in *Rhodosporidium toruloides* grown on single and mixed substrates. Microb Cell Fact 14, 36. https://doi.org/10.1186/s12934-015-0217-5

Braunwald, T., Schwemmlein, L., Graeff-Hönninger, S., French, W. T., Hernandez, R., Holmes, W. E., & Claupein, W. (2013). Effect of different C/N ratios on carotenoid and lipid production by *Rhodotorula glutinis*. Applied Microbiology and Biotechnology, 97(14), 6581–6588. https://doi.org/10.1007/s00253-013-5005-8

Carotenoids. (2021, January 1). Linus Pauling Institute. https://lpi.oregonstate.edu/mic/dietary-factors/phytochemicals/carotenoids

Castañeda, M. T., Nuñez, S., Garelli, F., Voget, C., & De Battista, H. (2018). Comprehensive analysis of a metabolic model for lipid production in *Rhodosporidium toruloides*. Journal of Biotechnology, 280, 11–18. https://doi.org/10.1016/j.jbiotec.2018.05.010

Fakankun I., Mirzaei M., Levin D.B. (2019) Impact of Culture Conditions on Neutral Lipid Production by Oleaginous Yeast. In: Balan V. (eds) Microbial Lipid Production. Methods in Molecular Biology, vol 1995. Humana, New York, NY. https://doi.org/10.1007/978-1-4939-9484-7_18

Fei, Q., O'Brien, M., Nelson, R., Chen, X., Lowell, A., & Dowe, N. (2016). Enhanced lipid production by *Rhodosporidium toruloides* using different fed-batch feeding strategies with lignocellulosic hydrolysate as the sole carbon source. Biotechnology for Biofuels, 9(1). https://doi.org/10.1186/s13068-016-0542-x

Johnson, V., Singh, M., Saini, V. S., Sista, V. R., & Yadav, N. K. (1992). Effect of pH on lipid accumulation by an oleaginous yeast:*Rhodotorula glutinis* IIP-30. World Journal of Microbiology & Biotechnology, 8(4), 382–384. https://doi.org/10.1007/bf01198749

Leif, R. C. (1986). Practical flow cytometry, by Howard M. Shapiro. Alan R. Liss, New York, 1985, 295 pages. Cytometry, 7(1), 111–112. https://doi.org/10.1002/cyto.990070119

Li, Y., Zhao, Z., Bai, F., (2007). High-density cultivation of oleaginous yeast *Rhodosporidium toruloides* Y4 in fed-batch culture, Enzyme and Microbial Technology, 41: 312-317. https://doi.org/10.1016/j.enzmictec.2007.02.008

Mondala, A. H., Hernandez, R., French, T., McFarland, L., Santo Domingo, J. W., Meckes, M., Ryu, H., & Iker, B. (2011). Enhanced lipid and biodiesel production from glucose-fed activated sludge: Kinetics and microbial community analysis. AIChE Journal, 58(4), 1279–1290. https://doi.org/10.1002/aic.12655

Naghavi, F. (2014). Effect of Temperature, pH and Salinity on carotenoid production in *Rodotorula mucilaginosa*. AGRIS: International Information System for the Agricultural Science and Technology. https://agris.fao.org/agris-search/search.do?recordID=AE2019100739

Nawabi, P., Bauer, S., Kyrpides, N., and Lykidis, A. (2011). Engineering *Escherichia coli* for biodiesel production utilizing a bacterial fatty acid methyltransferase. Appl. Environ. Microbiol. 77, 8052–8061. https://doi.org/10.1128/aem.05046-11

Orth, J. D., Thiele, I., & Palsson, B. (2010). What is flux balance analysis? Nature Biotechnology, 28(3), 245–248. https://doi.org/10.1038/nbt.1614

Osorio-González, C. S., Hegde, K., Ferreira, P., Brar, S. K., Kermanshahipour, A., Soccol, C. R., & Avalos-Ramírez, A. (2019). Lipid production in *Rhodosporidium toruloides* using C-6 and C-5 wood hydrolysate: A comparative study. Biomass and Bioenergy, 130, 105355. https://doi.org/10.1016/j.biombioe.2019.105355

Osiro, K. O., Borgström, C., Brink, D. P., Fjölnisdóttir, B. L., & Gorwa-Grauslund, M. F. (2019). Exploring the xylose paradox in Saccharomyces cerevisiae through in vivo sugar signalomics of targeted deletants. Microbial Cell Factories, 18(1). https://doi.org/10.1186/s12934-019-1141-x

Ratledge, C. (1994). Yeasts, moulds, algae and bacteria as sources of lipids. SpringerLink. https://link.springer.com/chapter/10.1007/978-1-4615-2109-9_9?error=cookies_not_supported&code=299b8403-e415-416c-a764-b3d9025097c4

Ratledge, C. (2004). Fatty acid biosynthesis in microorganisms being used for Single Cell Oil production. Biochimie, 86(11), 807–815. https://doi.org/10.1016/j.biochi.2004.09.017

Ratledge, C., & Wynn, J. P. (2002). The Biochemistry and Molecular Biology of Lipid Accumulation in Oleaginous Microorganisms. Advances in Applied Microbiology, 1–52. https://doi.org/10.1016/s0065-2164(02)51000-5

Rocha, I., Maia, P., Evangelista, P., Vilaça, P., Soares, S., Pinto, J. P., Nielsen, J., Patil, K. R., Ferreira, E. C., & Rocha, M. (2010). OptFlux: an open-source software platform for in silico metabolic engineering. BMC Systems Biology, 4(1). https://doi.org/10.1186/1752-0509-4-45

Sen Gupta, S., & Ghosh, M. (2013). In VitroAntioxidative Evaluation ofα- andβ-Carotene, Isolated from Crude Palm Oil. Journal of Analytical Methods in Chemistry, 2013, 1–10. https://doi.org/10.1155/2013/351671

Shen, H., Zhang, X., Gong, Z., Wang, Y., Yu, X., Yang, X., & Zhao, Z. K. (2017). Compositional profiles of *Rhodosporidium toruloides* cells under nutrient limitation. Applied Microbiology and Biotechnology, 101(9), 3801–3809. https://doi.org/10.1007/s00253-017-8157-0

Shen, H., Zhang, X., Gong, Z., Wang, Y., Yu, X., Yang, X., & Zhao, Z. K. (2017). Compositional profiles of *Rhodosporidium toruloides* cells under nutrient limitation. Applied Microbiology and Biotechnology, 101(9), 3801–3809. https://doi.org/10.1007/s00253-017-8157-0

Shi, S., & Zhao, H. (2017). Metabolic Engineering of Oleaginous Yeasts for Production of Fuels and Chemicals. Frontiers in Microbiology, 8. https://doi.org/10.3389/fmicb.2017.02185

Sitepu,I., Selby,T., Lin, T., Zhu,S., Mills,K.B. (2014). Carbon source utilization and inhibitor tolerance of 45 oleaginous yeast species, Journal of Industrial Microbiology and Biotechnology, 417: 1061–1070. https://doi.org/10.1007/s10295-014-1447-y

Somashekar, D., & Joseph, R. (2000). Inverse relationship between carotenoid and lipid formation in *Rhodotorula gracilis* according to the C/N ratio of the growth medium. World Journal of Microbiology and Biotechnology, 16(5), 491–493. https://doi.org/10.1023/a:1008917612616

Steinbüchel, A. (1991). Recent advances in the knowledge of the metabolism of bacterial polyhydroxyalkanoic acids and potential impacts on the production of biodegradable thermoplastics. Acta Biotechnologica, 11(5), 419–427. https://doi.org/10.1002/abio.370110504

Xie, D., Jackson, E. N., & Zhu, Q. (2015). Sustainable source of omega-3 eicosapentaenoic acid from metabolically engineered *Yarrowia lipolytica*: from fundamental research to commercial production. Applied Microbiology and Biotechnology, 99(4), 1599–1610. https://doi.org/10.1007/s00253-014-6318-y

Yaegashi, J., Kirby, J., Ito, M., Sun, J., Dutta, T., Mirsiaghi, M., Sundstrom, E. R., Rodriguez, A., Baidoo, E., Tanjore, D., Pray, T., Sale, K., Singh, S., Keasling, J. D., Simmons, B. A., Singer, S. W., Magnuson, J. K., Arkin, A. P., Skerker, J. M., & Gladden, J. M. (2017). *Rhodosporidium toruloides*: a new platform organism for conversion of lignocellulose into terpene biofuels and bioproducts. Biotechnology for Biofuels, 10(1). https://doi.org/10.1186/s13068-017-0927-5

Zhang, S., Skerker, J.M., Rutter, C.D., Maurer, M.J., Arkin, A.P. and Rao, C.V. (2016), Engineering *Rhodosporidium toruloides* for increased lipid production. Biotechnol. Bioeng., 113: 1056-1066. https://doi.org/10.1002/bit.25864

APPENDIX

I. Characterization of *R. toruloides* shake flask experiments

Table A.1: Carbohydrate source experiment OD_{600} and sugar consumption data

Fermentation Time (hrs)	OD_Gly	Glycerol consumption (g/L)	OD_Xyl	Xylose Consumption (g/L)	OD_Glu	Glucose consumption (g/L)
0	0.45	19.63	0.47	18.23	0.41	22.25
3	0.41	19.57	0.51	18.43	0.53	22.14
6	0.39	19.93	0.53	18.49	0.74	22.31
9	0.34	19.94	0.61	19.08	1.45	21.65
12	0.36	20.08	1.37	18.64	1.61	21.81
24	0.31	20.71	2.32	17.22	6.88	16.93
32	0.31	20.88	5.55	14.74	9.37	13.25
48	1.60	20.81	10.47	6.76	14.72	6.91
54	2.51	19.72	11.62	4.45	15.50	4.39
72	9.61	14.12	16.47	0.05	16.10	0

Table A.2: Temperature variance experiment OD_{600} and glucose consumption data

Fermentation Time (hrs)	OD 36°C	Glu_36 (g/L)	OD 33°C	Glu_33 (g/L)	OD 27°C	Glu_27 (g/L)
0	0.41	22.13	0.43	21.66	0.42	21.61
3	0.53	21.09	0.59	21.68	0.58	21.61
6	0.83	20.99	0.99	21.53	0.83	21.39
9	2.07	20.70	2.575	20.90	1.82	21.38
12	2.79	20.04	3.59	19.53	2.53	20.06
24	6.08	14.75	6.81	14.20	7.62	13.85
32	6.72	13.06	10.72	9.28	11.67	9.89
48	6.95	10.10	8.45	6.70	14.50	4.20
54	7.42	9.30	10.17	4.12	14.35	2.39
72	7.90	4.36	10.40	0	16.02	0

Table A.3: pH variance experiment OD_{600} and glucose consumption data

Fermentation Time (hrs)	OD_6.5	Glucose_6.5 (g/L)	OD_4.5	Glucose_4.5 (g/L)	OD_4.0	Glucose_4.0 (g/L)
0	0.38	19.50	0.37	19.47	0.38	19.21
3	0.49	20.05	0.56	19.65	0.43	19.57
6	0.70	19.01	0.64	19.51	0.59	19.34
9	1.30	19.97	1.06	19.47	0.91	19.44
12	2.54	19.10	2.40	18.69	1.96	18.66
24	11.66	9.89	8.98	11.80	6.93	12.93
32	18.50	3.35	11.15	9.62	8.02	11.38
48	23.75	0	17.00	3.59	10.40	7.53
54	23.15	0	18.45	2.25	12.35	5.94
72	23.35	0	17.55	0.02	13.95	1.69

Table A.4: Biomass yield for characterization experiments at different carbohydrate sources, temperature and pH values

Experiment	Xf (g/L)	Xo (g/L)	Sf (g/L)	So (g/L)	Ysx (g/g)
Glucose	13.60	0.35	0.00	22.25	0.60
Xylose	14.59	0.42	0.05	18.23	0.78
36°C	8.49	0.45	4.36	22.14	0.45
33°C	11.11	0.46	0.00	21.66	0.49
27°C	13.72	0.36	0.00	21.61	0.62
6.5 pH	16.51	0.27	0.00	19.50	0.83
4.5 pH	13.22	0.28	0.02	19.47	0.67
4.0 pH	10.71	0.29	1.69	19.20	0.59

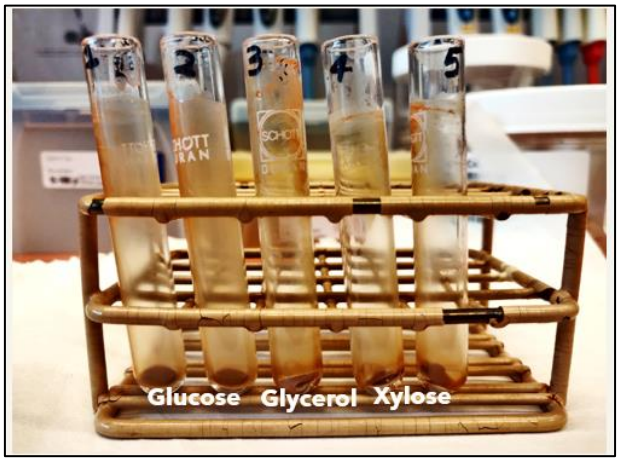

Fig A.1 : Dried *R. toruloides* cells after 72 hours of growth in different carbon sources

II. Nitrogen Limitation shake flask experiments

Table B.1: C:N 20 and 40 experiment OD_{600}, glucose, and ammonia consumption data

Fermentation Time (hrs)	OD_20	Ammonia_20 (g/L)	Glucose_20 (g/L)	OD_40	Ammonia_40 (g/L)	Glucose_40 (g/L)
0	0.39	0.63	20.66	0.46	0.3597	22.10
3	0.51	0.78	20.54	0.54	0.1014	22.17
6	0.75	0.57	20.40	0.85	0.1045	22.15
9	1.40	0.54	20.39	1.76	0.1020	21.60
12	3.16	0.52	18.92	3.32	0.1001	20.20
24	10.06	0.43	10.98	9.52	0.0592	13.37
32	12.72	0.23	6.82	9.85	0.0302	9.35
48	16.65	0.22	0.60	13.50	0.0132	2.48
54	20.40	0.18	0	15.75	0.0003	0.80
72	20.10	0.20	0	16.20	0.0000	0

Table B.2: C:N 80 and 100 experiment OD_{600}, glucose, and ammonia consumption data

Fermentation Time (hrs)	OD_80	Ammonia_80 (g/L)	Glucose_80 (g/L)	OD_100	Ammonia_100 (g/L)	Glucose_100 (g/L)
0	0.43	0.1777	22.36	0.44	0.0888	22.52
3	0.53	0.0994	22.52	0.53	0.0809	22.41
6	0.92	0.1035	22.43	0.93	0.0825	22.03
9	1.88	0.1002	21.85	1.98	0.0529	21.84
12	3.77	0.0734	20.46	3.65	0.0005	20.52
24	9.85	0.0003	13.40	11.62	0.0003	13.86
32	11.00	0.0000	9.25	11.75	0.0000	10.13
48	15.80	0.0000	1.84	20.70	0.0000	1.51
54	19.85	0.0000	0.67	25.90	0.0000	0.22
72	21.45	0.0000	0	27.45	0.0000	0

Table B.3: Glucose and ammonium salt consumption yields at different C:N ratios

	Exponential Growth Phase (3h-12h)					Nitrogen Consumption (0h-72h)				
Experiment	**Xf (g/L)**	**Xo (g/L)**	**Sf (g/L)**	**So (g/L)**	**Ysx (g/g)**	**Sf (g/L)**	**So(g/L)**	**Nf (g/L)**	**No (g/L)**	**Ysn (g/g)**
C:N 20	1.20	0.19	18.92	20.55	0.62	20.67	0.00	0.2043	2.568	0.11
C:N 40	1.35	0.22	20.2045	22.17	0.58	22.10	0.00	0	1.452	0.07
C:N 80	1.19	0.17	20.47	22.52	0.50	22.36	0.00	0	1.019	0.05
C:N 100	1.11	0.16	20.53	22.41	0.50	22.52	0.00	0	0.692	0.03

III. Fatty Acid profile for shake flask and batch bioreactor experiments

Table C.1: Fatty Acid profiles for nitrogen limitation and bioreactor experiments

Experiment	Unknown C 10	Methyl Dodecanoate C 12:0	Unknown C12	Methyl Myristate C14:0	Unknown C 14	Methyl Palmitate C 16:0	Unknown C 16	Methyl Stearate C18:0	Methyl Arachidate C20:0	Methyl Behenate C22:0	SUM
C:N40	3.92%	0.00%	0.00%	0%	0.00%	4.80%	7.33%	3.66%	0.00%	0.00%	19.72 %
C:N80	3.48%	0.00%	0.00%	0%	0.00%	5.82%	8.55%	4.34%	0.00%	0.00%	22.20 %
C:N100	4.24%	0.00%	0.00%	0.33%	0.52%	9.18%	15.13%	6.54%	0.00%	0.00%	35.95 %
SIP Batch Bioreactor	3.22%	0.00%	0.00%	0.17%	0.23%	7.13%	11.37%	4.98%	0.00%	0.15%	27.25 %
OC Batch Bioreactor	4.23%	0.00%	0.00%	0.00%	0.00%	7.56%	12.93%	5.81%	0.00%	0.00%	30.53 %

IV. Batch bioreactor experiments

Table D.1: Glucose and ammonium salt consumption yields for the two reactors

Experiment	Xf (g/L)	Xo(g/L)	Sf(g/L)	So(g/L)	Ysx(g/g)	Nf(g/L)	No(g/L)	Ysn(g/g)
SIP	22.39	0.20	0.012	48.83	0.455	0	2.64	0.054
OC	17.44	0.15	10.49	53.14	0.405	0	1.75	0.041

Table D.2: Cell count and CDW (g/L) for different fementation time frames

Sample	Cell Dry Wt (g/L)	Cell Count (x10^6)	Sample	Cell Dry Wt (g/L)	Cell Count (x10^6)
SIP-6HR	0.30	1.26	**OC-6HR**	0.29	1.3
SIP-24HR	7.52	22.9	**OC-24HR**	5.03	13.5
SIP-48HR	14.56	32.4	**OC-48HR**	9.84	18.42
SIP-72HR	17.7	38.5	**OC-72HR**	12.44	29.5

Table D.3: Batch bioreactors OD_{600}, glucose, and ammonia consumption data

	SIP			OC		
Time (hrs)	**OD**	**Ammonia (g/l)**	**Glucose (g/L)**	**OD**	**Ammonia (g/l)**	**Glucose (g/L)**
0	0.61	0.400	48.83	0.44	0.366	53.15
3	0.63	0.346	48.78	0.50	0.356	52.01
6	0.85	0.364	49.26	0.78	0.378	52.18
9	1.49	0.341	48.61	1.48	0.348	51.47
12	2.89	0.301	48.03	3.46	0.268	48.70
24	14.64	0.017	36.57	13.15	0.000	40.87
32	27.28	0.003	29.70	20.50	0.000	34.82
48	38.93	0.000	17.92	29.13	0.000	24.97
54	47.10	0.000	13.21	37.05	0.000	21.93
72	64.80	0.000	1.68	41.70	0.000	13.16
78	64.45	0.000	0.01	49.70	0.000	10.49

V. Fed-Batch bioreactor experiments

Table E.1: Fed-batch bioreactors OD_{600}, glucose, and ammonia consumption data

	SIP			**OC**		
Time	**OD**	**Ammonia (g/L)**	**Glucose (g/L)**	**OD**	**Ammonia (g/L)**	**Glucose (g/L)**
0	0.6	0.406	18.34	0.54	0.377	20.88
6	0.9	0.370	20.11	0.77	0.371	20.53
12	4.1	0.098	18.08	3.39	0.183	18.91
24	26.4	0.010	2.54	15.01	0.003	6.84
30	31.0	0.000	0	15.48	0.000	4.94
48	45.6	0.000	0	26.53	0.000	1.38
72	77.4	0.000	0	44.85	0.000	0.00
78	65.4	0.000	0	46.80	0.000	0.02
96	71.2	0.000	0.36	58.30	0.000	1.55
168	90.6	0.000	15.97	65.57	0.000	8.06
192	70.5	0.000	24.02	70.65	0.000	13.66

Table E.2: Glucose and ammonium salt consumption yields for the two reactors

Experiment	**Xf (g/L)**	**Xo(g/L)**	**Sf(g/L)**	**So(g/L)**	**Ysx(g/g)**	**Nf(g/L)**	**No(g/L)**	**Ysn(g/g)**
SIP	8.70	0.19	2.54	18.3	0.54	0	2.86	0.182
OC	6.85	0.18	6.84	20.8	0.47	0	2.59	0.186

VII. OptFlux Simulation and Calculations

Table F.1: OptFlux simulation results for C:N 20, 40, 80 ,and 100

C:N 20 OptFlux Results

Consumption

Metabolite Id	Metabolite Name	Value
M_nh4_e	Ammonium	0.57
M_pi_e	Phosphate	0.45805
M_so4_e	Sulphate (extracellular)	0.01427
M_o2_e	O2 (extracellular)	4.08492
M_glc_e	Glucose	3.69

Production

Metabolite Id	Metabolite Name	Value
M_tag_c	Triacylglycerol (tripalmi...	0.15766
M_h_e	H+ (extracellular)	1.69918
M_h2o_e	water	9.17169
M_co2_e	Carbon dioxide	7.2807
M_cell_mass_c	Cell mass	0.09329

C:N 40 OptFlux Results

Consumption

Metabolite Id	Metabolite Name	Value
M_nh4_e	Ammonium	0.35
M_pi_e	Phosphate	0.28126
M_so4_e	Sulphate (extracellular)	0.00876
M_o2_e	O2 (extracellular)	4.27334
M_glc_e	Glucose	3.92

Production

Metabolite Id	Metabolite Name	Value
M_tag_c	Triacylglycerol (tripalmi...	0.20936
M_h_e	H+ (extracellular)	1.04336
M_h2o_e	water	10.04183
M_co2_e	Carbon dioxide	8.65559
M_cell_mass_c	Cell mass	0.05728

C:N 80 OptFlux Results

Consumption

Metabolite Id	Metabolite Name	Value
M_nh4_e	Ammonium	0.26
M_pi_e	Phosphate	0.20894
M_so4_e	Sulphate (extracellular)	0.00651
M_o2_e	O2 (extracellular)	4.45276
M_glc_e	Glucose	4.11

Production

Metabolite Id	Metabolite Name	Value
M_tag_c	Triacylglycerol (tripalmi...	0.23704
M_h_e	H+ (extracellular)	0.77506
M_h2o_e	water	10.65349
M_co2_e	Carbon dioxide	9.46068
M_cell_mass_c	Cell mass	0.04255

C:N 100 OptFlux Results

Consumption

Metabolite Id	Metabolite Name	Value
M_nh4_e	Ammonium	0.12
M_pi_e	Phosphate	0.09643
M_so4_e	Sulphate (extracellular)	0.003
M_o2_e	O2 (extracellular)	3.5949
M_glc_e	Glucose	3.34

Production

Metabolite Id	Metabolite Name	Value
M_tag_c	Triacylglycerol (tripalmi...	0.20759
M_h_e	H+ (extracellular)	0.35772
M_h2o_e	water	8.76421
M_co2_e	Carbon dioxide	8.0173
M_cell_mass_c	Cell mass	0.01964

Table F.2: OptFlux simulation results for batch and fed-batch SIP and OC bioreactors

Batch SIP OptFlux Results

Consumption

Metabolite Id	Metabolite Name	Value
M_nh4_e	Ammonium	0.2
M_pi_e	Phosphate	0.16072
M_so4_e	Sulphate (extracellular)	0.00501
M_o2_e	O2 (extracellular)	2.36722
M_glc_e	Glucose	2.17

Production

Metabolite Id	Metabolite Name	Value
M_tag_c	Triacylglycerol (tripalmi...	0.11487
M_h_e	H+ (extracellular)	0.5962
M_h2o_e	water	5.55157
M_co2_e	Carbon dioxide	4.76896
M_cell_mass_c	Cell mass	0.03273

Batch OC OptFlux Results

Consumption

Metabolite Id	Metabolite Name	Value
M_nh4_e	Ammonium	0.201
M_pi_e	Phosphate	0.16152
M_so4_e	Sulphate (extracellular)	0.00503
M_o2_e	O2 (extracellular)	3.90397
M_glc_e	Glucose	3.61

Production

Metabolite Id	Metabolite Name	Value
M_tag_c	Triacylglycerol (tripalmi...	0.21269
M_h_e	H+ (extracellular)	0.59918
M_h2o_e	water	9.38941
M_co2_e	Carbon dioxide	8.4084
M_cell_mass_c	Cell mass	0.0329

Fed-batch SIP OptFlux Results

Consumption

Metabolite Id	Metabolite Name	Value
M_nh4_e	Ammonium	0.175
M_pi_e	Phosphate	0.14063
M_so4_e	Sulphate (extracellular)	0.00438
M_o2_e	O2 (extracellular)	2.48878
M_glc_e	Glucose	2.29

Production

Metabolite Id	Metabolite Name	Value
M_tag_c	Triacylglycerol (tripalmi...	0.12714
M_h_e	H+ (extracellular)	0.52168
M_h2o_e	water	5.90069
M_co2_e	Carbon dioxide	5.16266
M_cell_mass_c	Cell mass	0.02864

Fed-batch OC OptFlux Results

Consumption

Metabolite Id	Metabolite Name	Value
M_nh4_e	Ammonium	0.101
M_pi_e	Phosphate	0.08116
M_so4_e	Sulphate (extracellular)	0.00253
M_o2_e	O2 (extracellular)	2.12177
M_glc_e	Glucose	1.964

Production

Metabolite Id	Metabolite Name	Value
M_tag_c	Triacylglycerol (tripalmi...	0.11708
M_h_e	H+ (extracellular)	0.30108
M_h2o_e	water	5.11801
M_co2_e	Carbon dioxide	4.60465
M_cell_mass_c	Cell mass	0.01653

VIII. Flow Cytometry Table

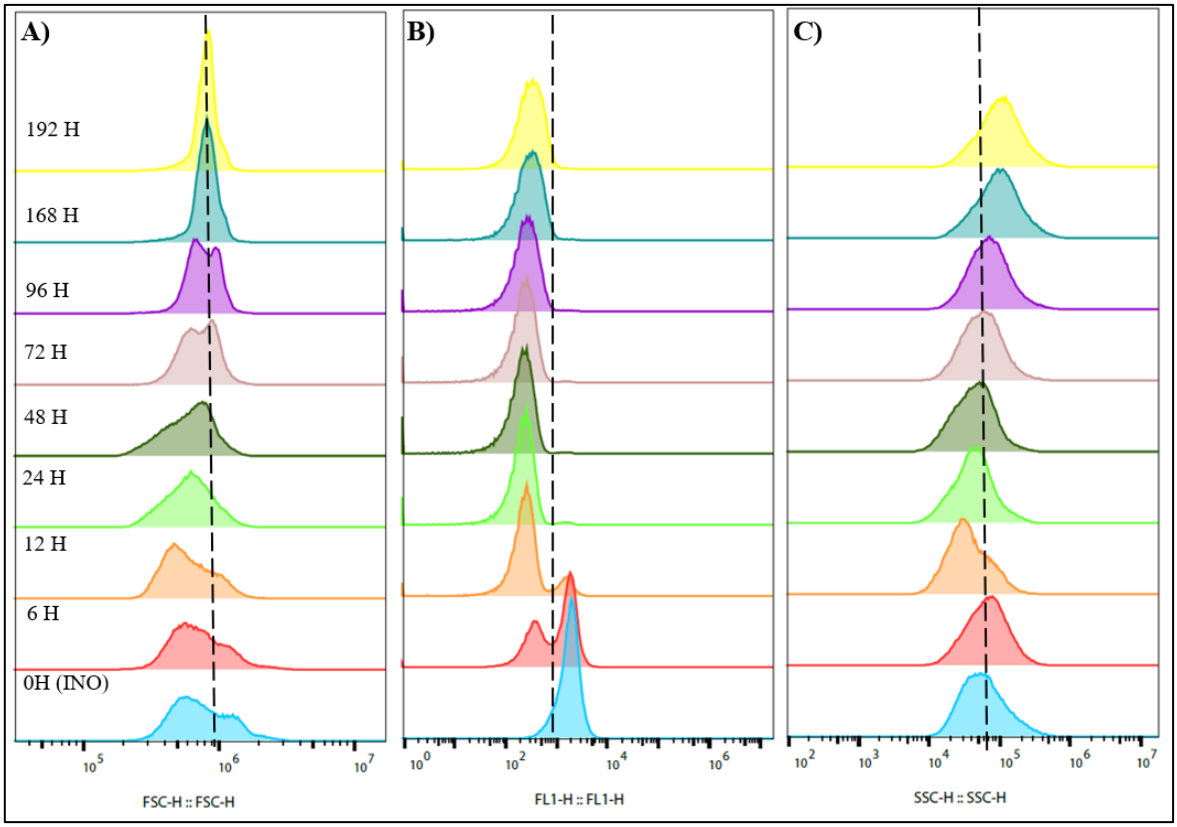

Fig G.1: Flow cytometry results for whole duration of OC, Old Control fed-batch fermentation. A) Forward scatter SIP fermentation; B) Scatter plots for filter FL1 for SIP; C) Side scatter for SIP

Table G.1: Geometric mean values for FSC-H, SSC-H FL1-H for SIP and OC reactors during fed-batch experiment

	SIP			OC		
Fermentation Time	**FL1-H**	**FSC-H**	**SSC-H**	**FL1-H**	**FSC-H**	**SSC-H**
0	1483	726000	58777	1751	746000	59092
6	765	721000	57419	901	714000	64964
12	291	623000	37450	265	597000	36057
24	159	628000	40380	192	608000	42218
48	172	681000	47942	177	599000	42807
72	169	760000	66466	200	718000	56253
96	187	785000	80063	223	764000	71022
168	229	802000	97270	270	805000	94824
192	239	806000	102162	292	799000	100205